

CHAPTER 14

Channel routing

D. L. Fread

*Hydrologic Research Laboratory,
National Weather Service, NOAA*

14.1. INTRODUCTION

Channel routing is a mathematical method (model) to predict the changing magnitude, speed, and shape of a flood wave as it propagates through waterways such as canals, rivers, reservoirs, or estuaries. The flood wave can emanate from precipitation runoff (rainfall or snowmelt), reservoir releases (spillway flows or dam-failures), and tides (astronomical and/or wind-generated).

Channel routing has long been of vital concern to man as he has sought to predict the characteristic features of a flood wave in his efforts to improve the transport of water through man-made or natural waterways and to determine necessary actions to protect life and property from the effects of flooding. Commencing with investigations as early as the seventeenth century, mathematical techniques to predict wave propagation have continually been developed. With the contribution of Saint-Venant in 1871, the basic theory for one-dimensional analysis of flood wave propagation was formulated; however, due to the mathematical complexity of Saint-Venant's theoretical equations, simplifications were necessary to obtain feasible solutions for the salient characteristics of the wave. Thereafter, a profusion of simplified flood routing methods appeared in the literature. It is only within the last 25 years, with the advent of high-speed electronic computers, that the complete Saint-Venant equations could be solved with varying degrees of feasibility.

14.1.1 Scope

In this chapter an overview of the various types of one-dimensional channel routing models is presented first. Then a detailed description is given of a particular routing model (FLDWAV) which is representative of the current state of the art. This model has wide applicability and feasible computational

requirements, and it is popular with many hydrologists and engineers. It also serves as a framework in which many flood routing complexities can be described and solution techniques presented. Selected applications of the model are presented. Finally, some suggestions are offered concerning future requirements and directions in channel routing development.

All mathematical notation used herein is defined when first presented.

14.2 SYNOPSIS OF CHANNEL ROUTING MODELS

Commencing with investigations by such eminent scientists as Newton (1687), Laplace (1776), Poisson (1816), Boussinesq (1871), and culminating in the one-dimensional equations of unsteady flow derived by Saint-Venant (1871), the theoretical foundation for channel routing was essentially achieved. The original Saint-Venant equations consist of the conservation of mass equation:

$$\frac{\partial(AV)}{\partial x} + \frac{\partial A}{\partial t} = 0 \quad (14.1)$$

and the conservation of momentum equation:

$$\frac{\partial V}{\partial t} + V \frac{\partial V}{\partial x} + g \left(\frac{\partial h}{\partial x} + S_f \right) = 0 \quad (14.2)$$

in which t is time, x is distance along the longitudinal axis of the waterway, A is cross-sectional area, V is velocity, g is the gravity acceleration constant, h is the water surface elevation above a datum, and S_f is the friction slope which may be evaluated using a steady flow empirical formula such as the Chezy or Manning equation. These are quasi-linear hyperbolic partial differential equations with two dependent parameters (V and h) and two independent parameters (x and t). A is a known function of h , and S_f is a known function of V and h . No analytical solutions can be obtained. Derivations of the Saint-Venant equations can be found in the following references: Stoker (1957), Chow (1959), Henderson (1966), Strelkoff (1969), and Liggett (1975).

Due to the complexities of the Saint-Venant equations, their solution was not feasible, and various simplified approximations of flood wave propagation continued to be developed. An excellent summary of such is presented by Miller and Yevjevich (1975). The simplified methods may be categorized as: (1) purely empirical; (2) linearization of the Saint-Venant equations; (3) hydrological, i.e., based on the conservation of mass and an approximate relation between flow and storage; and (4) hydraulic, i.e., based on the conservation of mass and a simplified form of the conservation of momentum equation. In recent years a fifth category of flood routing models, based on the complete Saint-Venant equations, have become economically feasible as a

- result of advances in computing equipment and improved numerical solution techniques. Following is a brief review of several models in each of the five categories.

14.3 EMPIRICAL MODELS

Some routing models are purely empirical, based on intuition and observations of past flood waves. Empirical models are limited to applications with sufficient observations of inflows and outflows of a reach of waterway to calibrate the essential empirical relationships or routing coefficients. They give their best results when applied to slowly fluctuating rivers with negligible lateral inflows and backwater effects. They require minimal computational resources; however, considerable effort can be required to derive the empirical parameters.

14.3.1 Lag models

Lag is defined as the difference in time between inflow and outflow within a routing reach. The successive average-lag method developed by Tatum (1940), assumes that there is a point downstream where the flow (I_2) at time (t_2) is equal to an average flow, i.e. $(I_1 + I_2)/2$. Tatum (1940) found that the number of successive averages occurring within a reach was approximately the time of travel of the wave divided by the reach length. Outflow (O) at the end of the reach is computed by:

$$O_{n+1} = C_1 I_1 + C_2 I_2 + \dots + C_{n+1} I_{n+1} \quad (14.3)$$

where n is the number of subreaches (successive averages) within the routing reach. The routing coefficients used in the method can be obtained via Tatum's approach or by trial and error using observed inflow and outflow hydrographs. The routing coefficients in equation (14.3) may also be obtained via a least-squares correlation of inflow and outflow hydrographs as described by Linsley *et al.* (1949). A similar lag model known as the progressive average-lag method was reported by Harris (1970).

14.3.2 Gauge relations

Empirical relationships which relate the flow at a downstream point to that at an upstream station known as gauge relations are described by Linsley *et al.* (1949). Gauge relations can be based on flow, water elevations, or a combination of each. The effect of lateral inflows is automatically contained in the empirical relation.

14.4 LINEARIZED MODELS

The complexity of the Saint-Venant equations has caused many scientists and engineers to simplify them in order to obtain solutions. The simplifications have been to either totally ignore the least important nonlinear terms and/or to linearize the remaining nonlinear terms in the equations. Given a sufficiently simplified form of the equations, they can be integrated analytically to obtain solutions of velocity and water surface elevation for any pair of (x,t) values at a relatively small expenditure of computational effort. Usually the most common simplifying assumptions are: (1) ignore the second term in equation (14.2); (2) constant cross-sectional area, usually rectangular; (3) constant channel bottom slope, often assumed to be zero; (4) the friction slope term is linearized with respect to velocity and depth; (5) no lateral inflow; and (6) the routed flood wave has a simple shape that is amenable to an analytical expression. These simplifications usually invoke severe limitations on the conditions for which the solution is valid. The applicability of a particular linearized model is limited by the assumptions in its derivation. The complete linearized model, Harley (1967), is the least restricted, although it is not appropriate when backwater effects exist due to the presence of tides, significant lateral inflows, dams, bridges, or cross-sectional irregularities.

14.4.1 Classical wave models

Neglecting lateral inflow, frictional resistance and nonlinear terms $V\partial A/\partial x$ and $V\partial V/\partial x$ in equations (14.1) and (14.2) respectively, the following classical linear wave equations may be obtained:

$$\frac{\partial^2 V}{\partial t^2} = gD \frac{\partial^2 V}{\partial x^2} \quad \text{and} \quad \frac{\partial^2 h}{\partial t^2} = gD \frac{\partial^2 h}{\partial x^2} \quad (14.4)$$

where D is the average depth. The analytical solutions of equations (14.4) have the following form (Abbott, 1966):

$$V = C_1(x - \sqrt{gD}t) + C_2(x + \sqrt{gD}t) \quad (14.5)$$

where C_1 and C_2 are functions determined by initial flow conditions and the boundary conditions.

Also, by assuming a rectangular cross-section, zero bottom slope, linearized resistance, and neglecting the $V\partial V/\partial x$ term, the following equation may be obtained after combining the resulting simplified forms of equations (14.1) and (14.2) and eliminating h ;

$$gD \frac{\partial^2 V}{\partial x^2} = \frac{\partial^2 V}{\partial t^2} + gC_0 \frac{\partial V}{\partial t} \quad (14.6)$$

in which C_0 is a constant depending on the linearized resistance term. Equation

(14.6) is in the form of the telegraph-equation which has been extensively studied (Dronkers, 1964).

14.4.2 Simple impulse response models

Linear systems theory has been used to develop routing techniques (Dooge, 1973). In this approach the routing model is assumed to be composed of linear reservoirs connected by linear channels. According to linear systems theory, any linear system is completely and uniquely characterized by its unit impulse response. By knowing the unit impulse response all possible system outputs may be determined for all possible inputs. The input-output relationship is defined by the convolution integral:

$$O(t) = \int_0^t I(t')H(t-t')dt' \quad (14.7)$$

in which $O(t)$ is the routed flow, $I(t)$ is the inflow, and $H(t-t')$ is the unit impulse response. The unit impulse response for a distributed linear reservoir was given by Maddaus (1969) as:

$$H_N(x,t) = \frac{1}{N} \sum_{m=1}^N \frac{e^{-(t-m\tau)/K}}{K\Gamma(m)} \left(\frac{t-m\tau}{K}\right)^{m-1} \dots t > m\tau \quad (14.8)$$

where N is the number of linear elements, $\Gamma(\)$ is the gamma function, K is the characteristic linear reservoir time constant, and τ is a time constant. The parameters, k and τ , are obtained by a fitting procedure described by Maddaus. A similar unit-response approach for routing through a single linear reservoir was reported by Sauer (1973). This approach is analogous to the unit hydrograph used by hydrologists to compute rainfall runoff. Also, it is related to the lag methods.

14.4.3 Complete linearized models

Linearized models of the complete Saint-Venant equations were developed by Lighthill and Whitham (1955) and Harley (1967). If equations (14.1) and (14.2) are rewritten for a unit-width channel and in terms of unit discharge (q') and depth (y), and then combined and linearized about a reference flow velocity ($V_0 = q_0/y_0$), the following linearized equation is obtained:

$$(gy_0^3 - V_0^2) \frac{\partial^2 q'}{\partial x^2} - 2V_0 \frac{\partial^2 q'}{\partial x \partial t} - \frac{\partial^2 q'}{\partial t^2} = 3gS_0 \frac{\partial q'}{\partial qx} + 2g \frac{S_0}{V_0} \frac{\partial q'}{\partial t} \quad (14.9)$$

in which S_0 is the channel bottom slope. Harley *et al.* (1970) obtained the following unit response function for equation (14.9):

$$H(x,t) = e^{-Px} \delta(t-x/C_1) + h'(x/C_1 - x/C_2) e^{sx-t} I[2h'm'] / m' \quad (14.10)$$

where:

$$C_1 = V_0 + \sqrt{gy_0} \quad (14.11)$$

$$C_2 = V_0 - \sqrt{gy_0} \quad (14.12)$$

$$F = V_0/\sqrt{gy_0} \quad (14.13)$$

$$P = S_0(2 - F)/[2y_0(F^2 + F)] \quad (14.14)$$

$$r = S_0V_0(2 + F^2)/(2y_0F^2) \quad (14.15)$$

$$s = S_0/(2y_0) \quad (14.16)$$

$$h' = S_0V_0[(4 - F^2)(1 - F^2)]^{1/2}/(4y_0F^2) \quad (14.17)$$

$$m' = [(t - x/C_1)(t - x/C_2)]^{1/2} \quad (14.18)$$

and $I[\]$ is a first-order Bessel function of the first kind and δ is the delta function. This model is similar to the diffusion analogy model developed by Hayami (Chow, 1959); however, it does not over-attenuate the flood wave as much as the simpler diffusion analogy model. The accuracy of the model is very dependent on the reference flow.

14.4.4 Multiple linearized models

Keefer and McQuivey (1974) presented an improved method for linearized models in which they introduced a multiple linearization technique for both the complete linearized model of Harley and the diffusion analogy model of Hayami (Chow, 1959); they concluded the latter was more practical.

14.5 HYDROLOGICAL MODELS

Significant river improvement projects in the early 1900s provided the impetus for development of an array of simplified flood routing methods. These have been termed hydrological models. They are based on the conservation of mass equation (14.1) written in the following form:

$$I - O = \Delta S/\Delta t \quad (14.19)$$

in which ΔS is the change in storage within the reach during a Δt time increment; the storage (S) is assumed to be related to inflow (I) and/or outflow (O), i.e.,

$$S = K[XI + (1 - X)O] \quad (14.20)$$

in which K is a storage constant with dimensions of time (seconds), and X is a weighting coefficient, $0 \leq X \leq 1$. All hydrological models are limited to

applications where the depth–discharge relation is single-valued. Thus backwater effects from tides, significant tributary inflow, dams or bridges are not considered by these models, nor are they well-suited for very mild sloping waterways where looped depth–discharge ratings may exist. Most hydrological models are also limited to applications where observed inflow–outflow hydrographs exist. When using the observed hydrographs to calibrate the routing coefficients, variations in flood wave shapes within the observed data set are not considered, and only the average wave shape is reflected in the fitted routing coefficients. Generally, the hydrological models have two parameters which can be calibrated to effectively reproduce the flood wave speed and its attenuated peak.

14.5.1 Storage routing models

Storage routing models attributed to Puls (1928) and Goodrich (1931) were developed by assuming X in equation (14.20) to be zero, i.e. storage is dependent only on outflow. Expressing equation (14.19) in centred finite difference form, the following reservoir routing model is obtained:

$$\frac{I_1 + I_2}{2} - \frac{O_1 + O_2}{2} = \frac{S_2 - S_1}{\Delta t} \quad (14.21)$$

which can be rearranged as:

$$\frac{2S_2}{\Delta t} + O_2 = I_1 + I_2 + \frac{2S_1}{\Delta t} - O_1 \quad (14.22)$$

which can be solved step-by-step for the left-hand side since O_1 and S_1 are known at time $t = 0$. An $S_2 = f(O_2)$ relationship obtained from observed inflow–outflow hydrographs allows the outflow (O_2) to be determined.

14.5.2 Muskingum model

If equation (14.20) with non-zero values for K and X is used for the storage relationship and this is substituted in equation (14.21), the following is obtained for computing O :

$$O_2 = C_1 I_2 + C_2 I_1 + C_3 O_1 + C_4 \quad (14.23)$$

where:

$$C_0 = K - KX + \Delta t/2 \quad (14.24)$$

$$C_1 = -(KX - \Delta t/2)/C_0 \quad (14.25)$$

$$C_2 = (KX + \Delta t/2)/C_0 \quad (14.26)$$

$$C_3 = (K - KX - \Delta t/2)/C_0 \quad (14.27)$$

$$C_4 = 0.5(q_1 + q_2) \Delta x \Delta t/C_0 \quad (14.28)$$

Equation (14.23), which has been expanded to include the effects of lateral inflow (q) along the Δx routing reach, is the widely used Muskingum routing model first developed by McCarthy (1935). The parameters K and X are determined from observed inflow–outflow hydrographs using any of the following techniques (Singh and McCann, 1980): (1) least-squares or its equivalent, the graphical method; (2) method of moments; (3) method of cumulants; and (4) direct optimization method. Among the many descriptions and variations of the Muskingum model are: Linsley *et al.* (1949); Nash (1959); Diskin (1967), Strupczewski and Kundzewicz (1980); and Dooge *et al.* (1982).

14.5.3 Muskingum–Cunge model

A significant improvement of the Muskingum model was developed by Cunge (1969). Cunge derived equation (14.23) using the assumption of a single-valued depth–discharge relation, the classical kinematic wave equation (see equation (14.43)), and applying a four-point implicit finite difference approximation technique. Equation (14.23) remains the same, but the following expressions for K and X are determined:

$$K = \Delta x/c \quad (14.29)$$

$$X = 0.5[1 - q_0/(cS_0 \Delta x)] \quad (14.30)$$

where $c = dQ/dA \quad (14.31)$

in which c is the kinematic wave speed corresponding to a unit-width reference discharge q_0 , Δx is the reach length and S_0 is the channel bottom slope. Equation (14.31) may be expressed in an alternative form, i.e.:

$$c = 1.27\beta S_0^{0.3}/(q_0^{0.4} n^{0.6}) \quad (14.32)$$

where: $\beta = 5/3 - 2/3 \frac{A_0}{B_0^2} dB/dy \quad (14.33)$

in which A_0 is the cross-sectional area corresponding to the total reference discharge (Q_0), B_0 is the channel width corresponding to Q_0 , y is the depth of flow, and the Manning equation is used to relate friction, depth and velocity. Depending on the cross-section shape, β may have values in the range, $1 < \beta \leq 5/3$. Selection of the appropriate time step (Δt) is given by;

$$\Delta t = T_r/M \quad (14.34)$$

where T_r is the time of rise of the inflow hydrograph and M is an integer whose value ranges from 5 to 20, depending on the extent of variation in the inflow

hydrograph. The selection of Δx affects the accuracy of the solution. It is related to Δt and is limited by the following inequality (Ponce, 1981):

$$\Delta x \leq 0.5 [c\Delta t + q_0/(cS_0)] \quad (14.35)$$

While the Muskingum–Cunge model does not require observed inflow–outflow hydrographs to establish the routing coefficients as required in the Muskingum model, best results are obtained if the wave speed (c) is determined from actual flow data. Also, the model is restricted to applications where backwater is not significant and channel rating curves do not have significant loops.

The Muskingum–Cunge model (Miller and Cunge, 1975; Weinmann and Laurenson, 1979) has created much interest in recent years as a highly versatile simplified routing model. Koussis (1978) and Ponce and Yevjevich (1978) have extended the model by using variable parameters c and B for temporally varying Q . Another model similar to the Cunge modification of the Muskingum model has been proposed by Koussis (1980).

14.5.4 Kalinin–Miljukov model

Another variation of the Muskingum model is the Kalinin–Miljukov model (Miller and Cunge, 1975), developed in 1958 in the USSR. This model has the following form:

$$O_2 = O_1 + (I_1 - O_1)K_1 + (I_2 - I_1)K_2 \quad (14.36)$$

where:

$$K_1 = 1 - e^{-c\Delta t/\Delta x} \quad (14.37)$$

$$K_2 = 1 - K_1\Delta x/(c\Delta t) \quad (14.38)$$

$$\Delta x = O/S_0(\Delta y/\Delta O) \quad (14.39)$$

in which $\Delta y/\Delta O$ is the slope of the depth–outflow rating curve. Equation (14.36) is identical to the Muskingum model if in the latter, $K = \Delta x/c$ and $X = 0$.

Another variation of the Muskingum model is the SSARR routing model (Rockwood, 1958) which Miller and Cunge (1975) show is similar to the Muskingum model with X assumed to be zero.

14.5.5 Lag and route model

Another hydrological storage routing model is the Lag and K model (Linsley *et al.*, 1949). First, the inflow is lagged and then the outflow (O_2) at time (t_2) is determined by substituting the relation $S_1 - S_1 = K(O_2 - O_1)$ in equation (14.21) and solving for O_2 , i.e.:

$$O_2 = [I_1 + I_2 - O_1(1 - 2K/\Delta t)]/(1 + 2K/\Delta t) \quad (14.40)$$

The extent of lag and the K parameter may be constants, or they can be functions of the inflow and outflow, respectively. Another lag and route model has been proposed by Quick and Pipes (1975).

14.6 SIMPLIFIED HYDRAULIC MODELS

The advent of computers made possible the development of another category of routing models based on equation (14.1) and various simplifications of equation (14.2). These models are classified as kinematic, diffusion, or quasi-steady depending on the terms retained in equation (14.2). The range of applicability of the kinematic and diffusion models has recently been treated by Ponce *et al.* (1978) who utilized a linear stability analysis of the finite difference form of the Saint-Venant equations. They compared wave attenuation factors and celerities and concluded that bottom slope and wave shape determine the range of their suitable applicability. In general, the steeper slopes associated with overland flow or steep streams with slow-rising floods are amenable to the use of kinematic models. The diffusion models have a wider range of applicability and can accommodate milder bottom slopes. However, there still remain many practical combinations of mild sloping channels and flood wave shapes that are not suitable for either diffusion or kinematic approximations and should be treated with the complete Saint-Venant equations.

14.6.1 Kinematic model

Interest in the kinematic model was initiated by Lighthill and Whitham (1955). There have been many forms of the kinematic model proposed; however, the basic assumption used in their derivation is that equation (14.2) can be simplified and expressed in the following form:

$$S_f - S_0 = 0 \quad (14.41)$$

in which $\partial h/\partial x = \partial y/\partial x - S_0$. Equation (14.41) implies that the momentum of the unsteady flow is assumed to be the same as that of steady uniform flow as described by the Chezy or Manning equation or a similar expression in which discharge is a single-valued function of depth, i.e. $\partial A/\partial Q = dA/dy = 1/c$ in which Q is discharge (flow) and c is the kinematic wave speed from equation (14.31) or (14.32). Also, since

$$\frac{\partial A}{\partial t} = \frac{\partial A}{\partial Q} \frac{\partial Q}{\partial t} \quad (14.42)$$

and $Q = AV$, equation (14.1) can be written as the classical kinematic equation, i.e.

$$\frac{\partial Q}{\partial t} + c \frac{\partial Q}{\partial x} = 0 \quad (14.43)$$

which can be solved by explicit or implicit finite difference methods, the latter being more efficient in most river applications. The kinematic wave model is limited to applications where single-valued depth–discharge ratings exist, and where backwater effects are insignificant, since in kinematic models flow disturbances can only propagate in the downstream direction. Also, the kinematic model modifies the flood wave through attenuation and dispersion via the errors inherent in the finite difference solution technique. The phenomenon of numerical damping merely mimics the actual physical damping of a flood wave since there is no mechanism in the basic kinematic equation to cause such damping. The kinematic wave models are very popular in applications to overland flow routing of precipitation runoff, e.g., Wooding (1965) and Woolhiser and Liggett (1967). Kinematic wave models have been used in channel routing by Harley *et al.* (1970) in the MIT catchment model and in the Hydrocomp model (Linsley, 1971).

14.6.2 Diffusion model

Another type of simplified hydraulic model is the diffusion model or zero-inertia model. The latter designation is derived from the basic assumption of this model that the inertia terms (first two) in equation (14.2) are insignificant. Thus, equation (14.2) takes the following form:

$$S_f + \partial h / \partial x = 0 \quad (14.44)$$

Equation (14.44) may be expressed in terms of channel conveyance K_c which is a single-valued function of elevation (h), i.e.,

$$Q = -K_c(h_x / |h_x|)(|h_x|)^{1/2} \quad (14.45)$$

where $h_x = \partial h / \partial x$. Equation (14.45) allows for upstream directed flows. Brakensiek (1965) solved equations (14.1) and (14.45) with a four-point centred implicit finite difference solution technique for reasons of computational efficiency. Harder and Armacost (1966) used an explicit finite difference solution technique for the diffusion routing model used by the Army Corps of Engineers (Harrison and Bueltel, 1973) on the Missouri River. This model is restricted to small time steps due to the numerical stability constraint given by:

$$\Delta t \leq B S_0^{1/2} \Delta x^2 / (K_c + S_0 \Delta x \Delta K_c / \Delta h) \quad (14.46)$$

in which B is the wetted top width of the channel. The nonlinear diffusion wave model is a significant improvement over the kinematic model because of the inclusion in equation (14.44) of the water surface slope term ($\partial h / \partial x$) of equation (14.1). This term allows the diffusion model to describe the attenuation (diffusion effect) of the flood wave. It also allows the specification of a boundary condition at the downstream extremity of the routing reach to account for backwater effects. It does not use the inertial terms (first two

terms) of equation (14.2) and, therefore, is limited to slow to moderately rising flood waves in channels of rather uniform geometry. Since inclusion of the inertial terms in an implicit (finite difference) solution of equation (14.44) in conjunction with equation (14.1) results in only a small increase in computational effort, the resulting dynamic model is generally preferred over the diffusion model due to the wider range of applicability of the dynamic wave model.

14.6.3 Quasi-steady model

A third type of simplified hydraulic model is the quasi-steady hydraulic model in which equation (14.1) is used along with equation (14.2) with all its terms except $\partial V/\partial t$. This simplification saves very little in computational effort and introduces more error than the simpler diffusion model. The quasi-steady model has been infrequently used, and its further use is not recommended.

14.7 COMPLETE HYDRAULIC MODELS

After the advent of high-speed computers, Stoker (1953) and Isaacson *et al.* (1954) first attempted to use the complete Saint-Venant equations for flood routing on the Ohio River. Since then, much effort has been expended in the development of the complete (dynamic wave) models. They are categorized according to the method of solution, i.e. direct or characteristic methods. In the direct methods finite difference approximations for the partial derivatives are substituted directly into equations (14.1) and (14.2), and solutions are obtained for incremental times (Δt) and distances (Δx) along the waterway. In the method of characteristics, the partial differential equations (14.1) and (14.2) are first transformed into an equivalent set of four ordinary differential equations which are then approximated with finite differences to obtain solutions. Dynamic models can be classified further as either explicit or implicit, depending on the type of finite difference scheme used in the solution. Explicit schemes transform the differential equations into a set of easily solved algebraic equations. However, implicit schemes transform the differential equations into a set of algebraic equations which must be solved simultaneously; the set of simultaneous equations may be either linear or nonlinear, the latter requiring an iterative solution procedure.

14.7.1 Characteristic models

Several methods of characteristic models were developed in the 1960s. Most were explicit, e.g. Liggett and Woolhiser (1967), Streeter and Wylie (1967), and Ellis (1970). Implicit characteristic models were reported by Amein (1966) and Wylie (1970). Characteristic models can have a curvilinear grid or

- a rectangular grid in the $x-t$ solution domain (Abbott, 1966). The former is not practical for application in natural waterways of irregular geometry. The latter, known as the Hartree method, requires interpolation formulae meshed within the finite difference solution procedure. These restrictions have tended to discourage the application of characteristic models for flood routing. The characteristic models for prismatic channels are based on the following four total differential equations:

$$dx/dt - V - \sqrt{gA/B} = 0 \quad (14.47)$$

$$dV/dt + \sqrt{gB/A} dy/dt + g(S_f - S_0) + q(V - v_x)/A - \sqrt{gB/A}q/B = 0 \quad (14.48)$$

$$dx/dt - V + \sqrt{gA/B} = 0 \quad (14.49)$$

$$dV/dt - \sqrt{gB/A} dy/dt + g(S_f - S_0) + q(V - v_x)/A + \sqrt{gB/A}q/B = 0 \quad (14.50)$$

Equations (14.47)–(14.50) are equivalent to the Saint-Venant partial differential equations (14.1) and (14.2) except that lateral inflow (q) has been included. The term v_x is the velocity of the lateral inflow in the x -direction along the axis of the waterway, A is cross-sectional area, B is cross-sectional top width, and y is depth.

14.7.2 Explicit models

Explicit finite difference models advance the solution of the Saint-Venant equations point by point along one time line in the $x-t$ solution domain until all the unknowns associated with that time line have been evaluated. Then, the solution is advanced to the next time line. In an explicit scheme the spatial derivatives and non-derivative terms are evaluated on the time line where the values of all variables are known. Only the time derivatives contain unknowns. Thus, in an explicit model, two linear algebraic equations are generated from the two Saint-Venant equations at each net point (node). Since the two equations can be solved directly for the unknowns, the equations are described as 'explicit'.

The development of explicit models began with the pioneering work of Stoker (1953). Among those who have reported on explicit models are Liggett and Woolhiser (1967), Martin and DeFazio (1969), and Strelkoff (1970). Dronkers (1969), Balloffet (1969) and Kamphuis (1970) applied explicit models to analyze tidal movement in estuaries. Garrison *et al.* (1969) and Johnson (1974) applied the explicit models for flood routing in rivers and reservoirs. Many variations of the explicit method have been developed, each based on a type of explicit finite difference scheme, e.g. the Stoker scheme, the diffusion scheme, and the leapfrog scheme. Descriptions and analyses of several explicit finite difference schemes have been given by Liggett and Cunge (1975).

In explicit models, equations (14.1) and (14.2) are usually expressed in the following form to enable an explicit solution of their finite difference approximations:

$$A \frac{\partial V}{\partial x} + V \frac{\partial A}{\partial x} + B_T \frac{\partial y}{\partial t} - q = 0 \quad (14.51)$$

$$\frac{\partial V}{\partial t} + V \frac{\partial V}{\partial x} + g \left(\frac{\partial y}{\partial x} - S_0 + S_f \right) + \frac{(V - v_x)q}{A} = 0 \quad (14.52)$$

in which B_T is the wetted top width of the total cross-sectional area (active and inactive or off-channel storage areas). Also, the effect of lateral inflow (q) is included in equations (14.51) and (14.52).

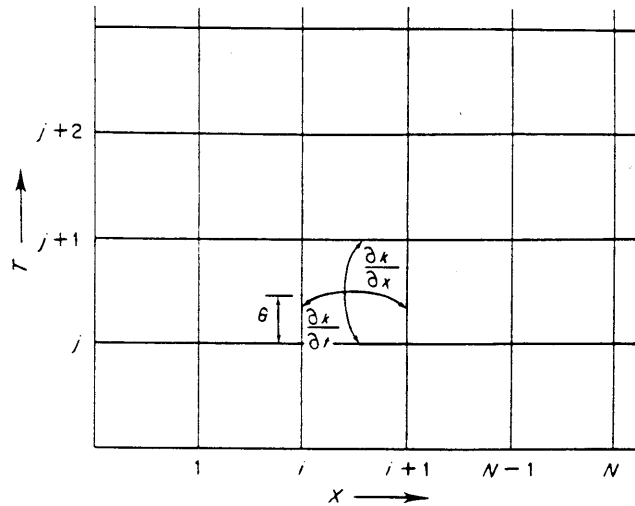
Explicit models, although relatively simple compared to implicit models, have a restriction in the size of the computational time step (Δt) in order to achieve numerical stability. In the Stoker scheme the maximum permissible time step (Δt) is given by the following inequality (Garrison *et al.*, 1969):

$$\Delta t \leq \Delta x / [V + \sqrt{gA/B} + gn^2 |V| \Delta x / (c_1 R^{4/3})] \quad (14.53)$$

in which n is the Manning roughness coefficient, $c_1 = 1.0$ in metric units and $c_1 = 2.21$ in English units, and R is the hydraulic radius. The first two terms in the denominator are associated with the well-known Courant condition for stability of explicit schemes in frictionless flow. The third term accounts for the effects of friction. This inequality, or some slight modification thereof, is representative of all explicit models. An inspection of equation (14.53) indicates that the computational time step is substantially reduced as the hydraulic depth (A/B) increases. Thus, in large rivers it is not uncommon for time steps on the order of a few minutes or even seconds to be required for numerical stability even though the flood wave may be very gradual, having a duration in the order of weeks. Such small time steps cause the explicit method to be very inefficient in the use of computer time. Another disadvantage of explicit schemes is the requirement of equal Δx distance steps.

14.7.3 Implicit models

Implicit finite difference schemes advance the solution of the Saint-Venant equations from one time line to the next simultaneously for all points along the time line (the x -axis of the waterway) in the $x-t$ solution domain of Figure 14.1. Thus, in an implicit model, a system of $2N$ algebraic equations is generated when finite difference approximations of the Saint-Venant equations are applied simultaneously to the N cross-sections along the x -axis. The system of algebraic equations so generated may be either linear or nonlinear, depending on the way non-derivative terms are approximated.

Figure 14.1 Discrete $x-t$ solution domain

Implicit models were developed because of the limitations on the size of the time step required for numerical stability of explicit models. The use of implicit models was suggested by Isaacson *et al.* (1956) and first appeared in the literature in the early 1960s with the work of Preissmann (1961) and Vasiliev *et al.* (1965). Later, Abbott and Ionescu (1967), Baltzer and Lai (1968), Dronkers (1969), Amein and Fang (1970), Kamphuis (1970), Contractor and Wiggert (1972), Quinn and Wylie (1972), Fread (1973), Chaudhry and Contractor (1973), Greco and Panattoni (1975), Amein and Chu (1975), Chen and Simons (1975), Bennett (1975), and Fread (1976), were among those reporting their research with implicit methods.

Analysis of the numerical stability and accuracy of various implicit schemes has been reported by Cunge (1966), Abbott and Ionescu (1967), Dronkers (1969), Gunaratnam and Perkins (1970), Fread (1974), Liggett and Cunge (1975), and Ponce and Simons (1977). Within the simplifications required in making the numerical stability analyses, the various implicit methods were found to be unconditionally linearly stable, i.e. the simplified linearized versions of the Saint-Venant equations were numerically stable independent of the size of the time or distance steps. However, Chaudhry and Contractor (1973), Fread (1974) and Cunge (1975a) found that instability could occur for the implicit schemes if the time steps were too large and the x -derivative terms were not sufficiently weighted towards the future time line when modelling rapidly varying transients. Also, time steps are restricted in size for reasons of accuracy; Δt is found to depend upon the shape of the wave, the Courant condition, the Δx step size, and the type of implicit scheme used. Nonlinearities

due to irregular cross-sections having widths that vary rapidly in the x -direction along the waterway or in the vertical direction can also cause numerical instabilities.

Implicit models are computationally more complex than explicit models. Depending on the type of implicit scheme (linear or nonlinear), the number of computations during a time step are several times greater than that of an explicit scheme. This extra computational requirement is very much greater if the method of solving the system of simultaneous equations is not efficient by taking advantage of the banded-structure of the coefficient matrix of the system of equations. Efficient solution techniques include the following: (1) a compact penta-diagonal elimination method described by Fread (1971) which makes use of the banded structure of the coefficient matrix of the system of equations, or (2) the double-sweep method developed in Europe (Liggett and Cunge, 1975). If the implicit scheme is linear, only one solution of the system of equations is required at each time step. However, if the implicit scheme is nonlinear, an iterative solution is necessary, and this requires one or more solutions of the system of equations at each time step. The use of the Newton-Raphson iterative method for nonlinear systems of equations (Amein and Fang, 1970) provides a very efficient solution if selected convergence criteria are practical. If the Newton-Raphson method is applied only once, the nonlinear implicit model is essentially equivalent to the linearized implicit models with respect to computational effort and performance.

Nonlinear implicit methods can be based on the conservation form of the Saint-Venant equations including lateral flow q (inflow is positive, outflow is negative) and off-channel (inactive flow) storage area A_0 , with dependent variables discharge (Q) and water elevation (h), i.e.,

$$\frac{\partial Q}{\partial x} + \frac{\partial(A + A_0)}{\partial t} - q = 0 \quad (14.54)$$

$$\frac{\partial Q}{\partial t} + \frac{\partial(Q^2/A)}{\partial x} + gA \left(\frac{\partial h}{\partial x} + S_f \right) + L = 0 \quad (14.55)$$

where $L = -qv_x$ for lateral inflow, $L = -qQ/A$ for bulk lateral outflow, and $L = -qQ/(2A)$ for seepage lateral outflow. An important advantage of equations (14.54) and (14.55) when they are expressed in finite difference form is their ability to accurately describe steep-fronted waves in waterways of non-prismatic geometry.

Linear implicit methods often utilize an expanded form of equations (14.54) and (14.55) such as that used by Chen and Simons (1975), i.e.

$$\frac{\partial Q}{\partial x} + B_T \frac{\partial y}{\partial t} - q = 0 \quad (14.56)$$

$$\frac{\partial Q}{\partial t} + 2 \frac{Q}{A} \frac{\partial Q}{\partial x} - \frac{Q^2}{A^2} \left[B \frac{\partial y}{\partial x} + \left(\frac{\partial \bar{A}}{\partial x} \right) \right] + gA \left(\frac{\partial y}{\partial x} - S_0 + S_f \right) + L = 0 \quad (14.57)$$

in which B_T is the total top width (active and inactive), $(\partial \bar{A}/\partial x)$ is the variation of A with respect to x with the depth (y) held constant, and S_f is expanded in a Taylor series in order to linearize this highly nonlinear term, i.e.,

$$S_f^{t+\Delta t} = S_f^t + (\partial S_f/\partial Q)^t (Q^{t+\Delta t} - Q^t) + (\partial S_f/\partial y)^t (y^{t+\Delta t} - y^t) \quad (14.58)$$

in which the superscripts (t and $t + \Delta t$) indicate at which time line the term is evaluated. In linear methods the accuracy of the solution is quite dependent on the size of Δt if the flow is rapidly changing with time due to the assumption of linearity of flow throughout a time step.

Implicit schemes have generally been four-point, i.e., the conservation of mass and momentum equations have been applied to the flow existing between two adjacent cross-sections. The weighted four-point scheme allows a convenient flexibility in the placement of x -derivative and non-derivative terms between two adjacent time lines in the $x-t$ solution domain. The weighting factor must be equal to or greater than 1/2 to provide unconditional linear stability with respect to time step size, and the accuracy of the scheme generally decreases as the weighting factor approaches unity, i.e., when the terms are expressed entirely at the forward time line. A few six-point schemes have been proposed, e.g. Abbott and Ionescu (1967) and Vasiliev *et al.* (1965), but they have the disadvantage of requiring regular Δx intervals whereas the four-point schemes allow variable Δx spacing. Also, the six-point schemes treat the boundary conditions in a more complicated manner than the four-point schemes.

14.7.4 Finite element models

The method of finite elements (Gray *et al.*, 1977) can also be applied to the complete Saint-Venant equations, e.g. Cooley and Moin (1976). Although this method of solution is popular in two-dimensional unsteady flow models, it does not appear to offer any advantages over the four-point nonlinear implicit models for the Saint-Venant one-dimensional equations of unsteady flow. Also, the mathematical basis for finite element solution schemes is not as easily understood as the finite difference approach. It seems that the personal preference of the model developer is the determining factor in selection of finite element or finite difference solution methods for the Saint-Venant equations.

14.7.5 Two-dimensional models

The unsteady flow equations when formulated in the x -direction as in equations (14.1) and (14.2), and also in the horizontal direction perpendicular to

the x -axis, become two-dimensional equations which form the basis for an array of models summarized by Hinwood and Wallis (1975a,b) and Abbott (1976), Abbott and Cunge (1975), Grupert (1976), and the simplified models described by Cunge (1975b) and Vicens *et al.* (1975). These models are beyond the intended scope and have been omitted from consideration herein. They are considerably more expensive to calibrate and execute on high-speed computers than the one-dimensional models. They are often used as an alternative modelling approach whenever a large amount of flow information is desired in complex unsteady flows associated with oceans and bays and water quality prediction therein and in estuarial networks.

14.8 MODEL SELECTION

Channel routing has been an important type of engineering analysis, and this importance, along with its inherent complexity, have resulted in the proliferation of routing models. The literature abounds with a wide spectrum of usable and reasonably accurate mathematical models for channel routing when each is used within the bounds of its limitations.

The selection of a channel routing model for a particular application is influenced by the relative importance one places on the following factors: (1) model accuracy; (2) the accuracy required in the application; (3) the type and availability of required data; (4) the available computational facilities; (5) the computational costs; (6) the extent of flood wave information desired; (7) one's familiarity with a given model; (8) the extent of documentation, range of applicability, and availability of a 'canned' or packaged routing model; (9) the complexity of the mathematical formulation if the routing model is to be totally developed from 'scratch' (coded for computer); and (10) one's capability and time available to develop a particular type of routing model. Taking all factors into consideration, and recognizing that each application may change the relative importance of each factor, it is apparent that there is no universally superior routing model.

In the absence of significant backwater effects, the hydrological storage routing models offer the advantage of simplicity. They hydrological models have two parameters which can be calibrated to effectively reproduce the simple characteristics of a flood wave such as its celerity and crest attenuation. The accuracy considerations restrict the hydrological and kinematic models to applications where the depth-discharge relation is essentially single-valued. Following the analysis of Ponce and Simons (1977), and Ponce *et al.* (1978) approximate criteria for their acceptable range of application can be formulated. For kinematic-type models including the Muskingum model, the following criterion will restrict routing errors to less than about 5 per cent:

$$T_r S_0^{1.6} / (q_0^{0.2} n^{1.2}) \geq 0.014 \quad (14.59)$$

A similar criterion for diffusion-type models including the Muskingum–Cunge model is:

$$T_r S_0^{1.15} / (q_0 n)^{0.3} \geq 0.0003 \quad (14.60)$$

in which T_r is time of rise (hours) of the inflow hydrograph, S_0 is the channel slope, q_0 is a unit-width reference discharge, and n is the Manning coefficient.

Inspection of equations (14.59) and (14.60) reveals the importance of the parameters, T_r and S_0 . Also it is apparent that the diffusion models are applicable for a wider range of bottom slopes and hydrographs than the kinematic models. In instances of a gently sloping channel and rapidly rising flood wave, when the combination of S_0 and T_r becomes small enough that equation (14.60) cannot be satisfied, the complete hydraulic (dynamic wave) models are required. The simple Muskingum–Cunge model can be used effectively in many applications where equation (14.60) is satisfied and backwater effects are not significant. However, as the trend continues for increasing computational speed and storage capabilities of computers at decreasing costs, accessibility to inexpensive computational resources should increase the feasibility of using the dynamic wave models for a wider range of applications.

Among the models reviewed, the hydraulic models based on the complete Saint-Venant equations have the capability to correctly simulate the widest spectrum of wave types and waterway characteristics. Since the dynamic wave models contain only one calibration parameter (the roughness coefficient), they are very amenable to the calibration process. Also, since the roughness coefficient can be estimated with some degree of accuracy from inspection of waterways or, better still, from minimal depth–discharge data, any of the hydraulic flood routing models or the Muskingum–Cunge model can be used when there is a scarcity of pertinent inflow–outflow observations such as in the case of ungauged rivers or proposed man-made changes to waterways. The hydraulic (dynamic wave) models are preferred over all other models when: (1) the backwater effect is important due to tides, significant tributary inflows, dams, and/or bridges; and (2) the upstream propagation of waves can occur from large tides and storm surges or very large tributary inflows. The implicit dynamic wave model is the most efficient and versatile, although the most complex, of the complete hydraulic models. A detailed description of such a model follows.

14.9 STRUCTURE OF THE DYNAMIC WAVE MODEL (FLDWAV)

The FLDWAV model is a synthesis of two widely used models, DWOPER (Fread, 1978) and DAMBRK (Fread, 1980). In addition, FLDWAV has significant modelling capabilities not available in either of the other models. FLDWAV is a generalized dynamic wave model for one-dimensional unsteady flows in a single or branched waterway. It is based on an implicit (four-point,

nonlinear) finite difference solution of the Saint-Venant equation. The following special features are included in FLDWAV: variable Δt and Δx computational intervals; irregular cross-sectional geometry; off-channel storage; roughness coefficients which vary with discharge or water surface elevation, and distance along the waterway; capability to generate linearly interpolated cross-sections and roughness coefficients between input cross-sections; automatic computation of initial steady flow and water elevations at all cross-sections along the waterway; external boundaries of discharge or water surface elevation time series (hydrographs), a single-valued or looped depth-discharge relation (tabular or computed); time-dependent lateral inflows (outflows); internal boundaries which enable the treatment of time-dependent dam failures, spillway flows, gate controls, bridge flows, bridge-embankment overtopping flow; short-circuiting of floodplain flow in a valley with a meandering river; levee failure and/or overtopping; a special computational technique to provide numerical stability when treating flows which change from supercritical to subcritical or, conversely, with time and distance along the waterway; and an automatic calibration technique for determining the variable roughness coefficient by using observed hydrographs along the waterway.

FLDWAV is coded in FORTRAN IV and the computer program is of modular design with each subroutine requiring less than 64,000 bytes of storage. Overall program storage requirement is approximately 256,000 bytes. Program array sizes are variable with the size of each array set internally via the input parameters used to describe the particular unsteady flow application for which the model is being used. Input data to the program is free or fixed-format. Program output is user-selective and consists of tabular and/or graphical displays.

14.10 BASIC ALGORITHM

FLDWAV is based on an implicit finite difference solution of the conservation form of the Saint-Venant equations of unsteady flow. In their conservation form, the equations consist of the conservation of mass equation, i.e.,

$$\frac{\partial Q}{\partial x} + \frac{\partial(A + A_0)}{\partial t} - q = 0 \quad (14.61)$$

and the conservation of momentum equation, i.e.,

$$\frac{\partial Q}{\partial t} + \frac{\partial(Q^2/A)}{\partial x} + gA \left(\frac{\partial h}{\partial x} + S_f + S_e \right) + L + W_f B = 0 \quad (14.62)$$

where:

$$S_f = \frac{n^2 |Q| Q}{2.21 A^2 R^{4/3}} = \frac{|Q| Q}{K_c^2} \quad (14.63)$$

$$S_e = \frac{K_e \partial(Q/A)^2}{2g \partial x} \quad (14.64)$$

$$W_f = C_w |V_r| V_r \quad (14.65)$$

in which x is distance along the longitudinal axis of the waterway, t is time, Q is discharge, A is active cross-sectional area, A_0 is inactive (off-channel storage) cross-sectional area, q is lateral inflow (positive) or outflow (negative), g is the gravity acceleration constant, h is water surface elevation, B is wetted top width of cross-section, L is the momentum effect of lateral inflow, S_f is friction slope computed from Manning's equation, n is the Manning n , R is the hydraulic radius approximated by (A/B) , K_c is the channel conveyance factor, S_e is the local loss slope, K_e is an expansion (negative) or contraction (positive) coefficient, W_f is the wind term, C_w is non-dimensional wind coefficient, V_r is the velocity of the wind (V_w) relative to the velocity of the channel flow where the acute angle between the wind direction and channel flow direction is ω and V_w is $(-)$ if aiding the flow.

In an implicit finite difference solution of equations (14.61) and (14.62), the continuous $x-t$ solution domain in which solutions of h and Q are sought is represented by a rectangular net of discrete points as shown in Figure 14.1. The net points (nodes) may be at equal or unequal intervals of Δt and Δx along the t and x axes, respectively. Each node is identified by a subscript (i) which designates the x position and a superscript (j) for the time line. A four-point weighted, implicit difference approximation is used to transform the nonlinear partial differential equations of Saint-Venant into nonlinear algebraic equations. The four-point weighted difference approximations are:

$$\frac{\partial K}{\partial t} = (K_i^{j+1} + K_{i+1}^{j+1} - K_i^j - K_{i+1}^j)/(2 \Delta t^j) \quad (14.66)$$

$$\frac{\partial K}{\partial x} = \theta/\Delta x_i (K_{i+1}^{j+1} - K_i^{j+1}) + (1 - \theta)/\Delta x_i (K_{i+1}^j - K_i^j) \quad (14.67)$$

$$K = 0.5\theta(K_i^{j+1} + K_{i+1}^{j+1}) + 0.5(1 - \theta)(K_i^j + K_{i+1}^j) \quad (14.68)$$

where K is a dummy parameter representing any variable in the above differential equations, θ is a weighting factor varying from 0.5 to 1, i is a subscript denoting the sequence number of the cross-section or Δx reach, and j is a superscript denoting the sequence number of the time line in the $x-t$ solution domain. A θ value of 0.5 is known as the 'box' scheme while $\theta = 1$ is the 'fully implicit' scheme. To insure unconditional linear numerical stability and provide good accuracy, θ values nearer to 0.5 are recommended (Fread, 1974). Accuracy decreases as θ departs from 0.5 and approaches 1.0. This effect becomes more pronounced as the time step size increases. FLDWAV allows θ to be an

input parameter. A value of 0.55 to 0.60 is often used to minimize loss of accuracy while avoiding weak or pseudo-instability which sometimes results when θ of 0.5 is used.

Substitution of the finite difference approximations defined by equations (14.66)–(14.68) into equations (14.61) and (14.62) for the derivatives and non-derivative terms and multiplying through by Δx_i yields the following difference equations:

$$\begin{aligned} & \theta(Q_{i+1}^{j+1} - Q_i^{j+1} - \bar{q}_i^{j+1} \Delta x_i) + (1 - \theta)(Q_{i+1}^j - Q_i^j - \bar{q}_i^j \Delta x_i) \\ & + 0.5 \Delta x_i / \Delta t^j [(A + A_0)_{i+1}^{j+1} + (A + A_0)_{i+1}^{j+1} - (A + A_0)_i^j \\ & - (A + A_0)_{i+1}^j] = 0 \end{aligned} \quad (14.69)$$

$$\begin{aligned} & 0.5 \Delta x_i / \Delta t^j (Q_{i+1}^{j+1} + Q_i^{j+1} - Q_i^j - Q_{i+1}^j) + \theta [(Q^2/A)_{i+1}^{j+1} - (Q^2/A)_i^{j+1} \\ & + g \bar{A}_i^{j+1} (h_{i+1}^{j+1} - h_i^{j+1} + \Delta x_i \bar{S}_{f_i}^{j+1} + \Delta x_i \bar{S}_{e_i}^{j+1}) \\ & + \Delta x_i (L + \bar{W}_f \bar{B})_{i+1}^{j+1}] + (1 - \theta) [(Q^2/A)_{i+1}^j - (Q^2/A)_i^j \\ & + g \bar{A}_i^j (h_{i+1}^j - h_i^j + \Delta x_i \bar{S}_{f_i}^j + \Delta x_i \bar{S}_{e_i}^j) + \Delta x_i (L + \bar{W}_f \bar{B})_i^j] = 0 \end{aligned} \quad (14.70)$$

$$\text{where:} \quad \bar{A}_i = 0.5(A_i + A_{i+1}) \quad (14.71)$$

$$\bar{B}_i = 0.5(B_i + B_{i+1}) \quad (14.72)$$

$$\bar{S}_{f_i} = \frac{\bar{n}_i^2 |\bar{Q}_i| \bar{Q}_i}{2.21 \bar{A}_i^2 R_i^{4/3}} = |\bar{Q}_i| \bar{Q}_i / \bar{K}_{c_i}^2 \quad (14.73)$$

$$\bar{Q}_i = 0.5(Q_i + Q_{i+1}) \quad (14.74)$$

$$R_i = \bar{A}_i / \bar{B}_i \quad (14.75)$$

$$\bar{K}_{c_i} = 0.5(K_{c_i} + K_{c_{i+1}}) \quad (14.76)$$

$$\bar{S}_{e_i} = K_{e_i} [(Q/A)_{i+1}^2 - (Q/A)_i^2] / (2g \Delta x_i) \quad (14.77)$$

$$\bar{W}_{f_i} = C_{w_i} |\bar{V}_{r_i}| \bar{V}_{r_i} \quad (14.78)$$

$$\bar{V}_{r_i} = \bar{Q}_i / \bar{A}_i - \bar{V}_{w_i} \cos \omega \quad (14.79)$$

$$\bar{L}_i = -(\bar{q} \bar{v}_{x_i}) \quad (\text{lateral inflow}) \quad (14.80)$$

$$L_i = -(\bar{q} \bar{Q} / \bar{A})_i \quad (\text{bulk lateral outflow}) \quad (14.81)$$

$$L_i = -(0.5 \bar{q} \bar{Q} / \bar{A})_i \quad (\text{seepage lateral outflow}) \quad (14.82)$$

The bar (—) above the variables represents the average of the variable over the reach length (Δx_i) between cross-sections i and $i + 1$. The subscript (i) associated with \bar{q} , \bar{v}_{x_i} , \bar{A} , \bar{B} , \bar{S}_f , \bar{Q} , \bar{S}_e , \bar{W}_f , \bar{V}_r , and \bar{V}_w represents the number

- of the reach (Δx_i) rather than the cross-section (node) number. Node numbers commence with 1 and terminate with N , while reach numbers commence with 1 and terminate with $(N - 1)$.

Equations (14.69) and (14.70) are nonlinear with respect to the unknowns h and Q at the points i and $i + 1$ on the $j + 1$ time line. All terms associated with the j th time line are known from either the initial conditions or previous computations. The initial conditions are values of h and Q at each computational point (node) along the x -axis for the first time line ($j = 1$).

Equations (14.69) and (14.70) are two nonlinear algebraic equations which cannot be solved in a direct (explicit) manner since there are four unknowns h and Q , at points i and $(i + 1)$ on the $(j + 1)$ time line and only two equations. However, if similar equations are formed for each of the $(N - 1)$ Δx reaches between the upstream and downstream boundaries, a total of $(2N - 2)$ equations with $2N$ unknowns results. (N denotes the total number of computational points or cross-sections.) Then prescribed boundary conditions, one at the upstream extremity of the waterway and one at the downstream extremity, provide the additional two equations required for the system to be determinate. The resulting system of $2N$ nonlinear equations with $2N$ unknowns is solved by the Newton-Raphson method which was first applied by Amein and Fang (1970) to an implicit nonlinear formulation of the Saint-Venant equations.

14.10.1 Newton-Raphson method

The Newton-Raphson method is a functional iterative technique to solve a system of nonlinear equations. The technique is derived from a Taylor series expansion of the nonlinear function in which all terms of second and higher order are neglected. The resulting algorithm is:

$$J'(X^k) \Delta X = -f(X^k) \quad (14.83)$$

in which X^k is a vector quantity, J' is the Jacobian (a coefficient matrix made up of the partial derivatives evaluated with X^k values), $f(X^k)$ is the nonlinear equation evaluated with X^k values, and ΔX is a vector containing the $2N$ unknowns. Equation (14.83) represents a system of equations in which the unknown vector ΔX is linear. Solution of equation (14.83) for the unknown ΔX is by an appropriate matrix inversion technique such as Gauss elimination. The ΔX vector actually represents the difference between an initial estimate of the true solution and an improved estimate, i.e.

$$\Delta X = X^{k+1} - X^k \quad (14.84)$$

in which k is the number of iteration, X^k is the initial estimate (guess) and X^{k+1} is the improved estimate. Convergence of the iterative solution is attained in usually one or two iterations when the ΔX vector containing the

unknown discharges (Q_i^{j+1} , Q_{i+1}^{j+1}) and water elevations (h_i^{j+1} , h_{i+1}^{j+1}) becomes less than convergence criteria which are specified for each application of FLDWAV. Typical values are 0.01 feet for convergence of water elevation (ϵ_h) while the convergence for the discharge is specified in ft^3/s according to the following relation;

$$\epsilon_Q = \epsilon_h \hat{B} \hat{V} \quad (14.85)$$

in which \hat{B} and \hat{V} are the representative channel width and velocity, respectively.

The convergence process depends on a good first estimate for the vector X^k . A reasonably accurate initial condition of the discharges and water elevations at $t=0$ provides the first X^k . Thereafter, X^k first estimate values can be obtained using extrapolated values from solutions at previous time steps according to the following algorithm:

$$X^k = X^{j-1} + (X^{j-1} - X^{j-2})\alpha' \Delta t^j / \Delta t^{j-1} \quad (14.86)$$

where Δt^j and Δt^{j-1} are values of time steps between the time lines corresponding to the solution vectors, X^j and X^{j-1} , respectively. The weighting factor α' can be specified over the range of zero to unity.

The Jacobian matrix, $J'(X^k)$, is composed of elements ($a_{i,k}$) located along the main-diagonal with two elements in rows 1 and $2N$ which represent the upstream and downstream external boundaries, respectively; and all other rows have four elements which represent the partial derivatives of equations (14.69) and (14.70) with respect to the four unknowns (Q_i^{j+1} , h_i^{j+1} , Q_{i+1}^{j+1} , h_{i+1}^{j+1}). Each adjacent pair of rows represent the application of equations (14.69) and (14.70) to each Δx_i reach along the waterway proceeding from the upstream to the downstream boundary.

Letting \hat{C} represent equation (14.69) and \hat{M} represent equation (14.70), their derivatives can be expressed as follows:

$$a_{i,k} = \partial \hat{C} / \partial Q_i^{j+1} = -\theta \quad (14.87)$$

$$a_{i,k+1} = \partial \hat{C} / \partial h_i^{j+1} = (B + B_0)_i^{j+1} 0.5 \Delta x_i / \Delta t^j \quad (14.88)$$

$$a_{i,k+2} = \partial \hat{C} / \partial Q_{i+1}^{j+1} = \theta \quad (14.89)$$

$$a_{i,k+3} = \partial \hat{C} / \partial h_{i+1}^{j+1} = (B + B_0)_{i+1}^{j+1} 0.5 \Delta x_i / \Delta t^j \quad (14.90)$$

$$\begin{aligned} a_{i+1,k} &= \partial \hat{M} / \partial Q_i^{j+1} = 0.5 \Delta x_i / \Delta t^j + \theta \{ -2(Q/A)_i^{j+1} \\ &\quad + g \bar{A}_i^{j+1} \Delta x_i [(\partial \bar{S}_f / \partial Q)_i^{j+1} + (\partial \bar{S}_e / \partial Q)_i^{j+1}] + \Delta x_i (\partial L / \partial Q)_i^{j+1} \} \end{aligned} \quad (14.91)$$

$$\begin{aligned}
a_{l+1,k+1} = \partial \tilde{M} / \partial h_i^{j+1} = & \theta \{ (BQ^2/A^2)_i^{j+1} + 0.5gB_i^{j+1}(h_{i+1}^{j+1} - h_i^{j+1}) \\
& + \Delta x_i \bar{S}_{f_i}^{j+1} + \Delta x_i \bar{S}_{e_i}^{j+1} \} + g\bar{A}_i^{j+1} [-1 + \Delta x_i (\partial \bar{S}_f / \partial h)_i^{j+1} \\
& + \Delta x_i (\partial \bar{S}_e / \partial h)_i^{j+1}] + \Delta x_i \{ (\partial L / \partial h)_i^{j+1} + 0.5(\bar{W}_f dB/dh)_i^{j+1} \}
\end{aligned} \quad (14.92)$$

$$\begin{aligned}
a_{l+1,k+2} = \partial \tilde{M} / \partial Q_{i+1}^{j+1} = & 0.5 \Delta x_i / \Delta t^j + \theta \{ 2(Q/A)_i^{j+1} \\
& + g\bar{A}_i^{j+1} \Delta x_i [(\partial \bar{S}_f / \partial Q)_{i+1}^{j+1} + (\partial \bar{S}_e / \partial Q)_{i+1}^{j+1}] + \Delta x_i (\partial L / \partial Q)_{i+1}^{j+1} \}
\end{aligned} \quad (14.93)$$

$$\begin{aligned}
a_{l+1,k+3} = \partial \tilde{M} / \partial h_{i+1}^{j+1} = & \theta \{ (-BQ^2/A^2)_{i+1}^{j+1} + 0.5gB_{i+1}^{j+1}(h_{i+1}^{j+1} - h_i^{j+1}) \\
& + \Delta x_i \bar{S}_{f_i}^{j+1} + \Delta x_i \bar{S}_{e_i}^{j+1} \} + g\bar{A}_i^{j+1} [1 + \Delta x_i (\partial \bar{S}_f / \partial h)_{i+1}^{j+1} \\
& + \Delta x_i (\partial \bar{S}_e / \partial h)_{i+1}^{j+1}] + \Delta x_i \{ (\partial L / \partial h)_{i+1}^{j+1} + 0.5(\bar{W}_f dB/dh)_{i+1}^{j+1} \}
\end{aligned} \quad (14.94)$$

$$\text{where:} \quad \partial \bar{S}_f / \partial Q = \bar{S}_f (1/\bar{Q} + 1/\bar{n} \Delta \bar{n} / \Delta \bar{Q}) \quad (14.95)$$

$$\partial \bar{S}_f / \partial h = 2\bar{S}_f \left[\frac{d\bar{n}/dh}{\bar{n}} - \frac{5B}{6\bar{A}} + \frac{dB/dh}{3\bar{B}} \right] = \frac{-\bar{S}_f dK_c/dh}{\bar{K}_c} \quad (14.96)$$

$$dB/dh = \Delta B / \Delta h \quad (14.97)$$

$$d\bar{n}/dh = 0.5 \Delta \bar{n} / \Delta \bar{h} \quad (14.98)$$

$$dK_c/dh = \Delta K_c / \Delta h \quad (14.99)$$

$$(\partial \bar{S}_e / \partial Q)_i^{j+1} = [-K_e Q / (g \Delta x A^2)]_i^{j+1} \quad (14.100)$$

$$(\partial \bar{S}_e / \partial Q)_{i+1}^{j+1} = [K_e Q / (g \Delta x A^2)]_{i+1}^{j+1} \quad (14.101)$$

$$(\partial \bar{S}_e / \partial h)_i^{j+1} = [K_e Q^2 B / (g \Delta x A^3)]_i^{j+1} \quad (14.102)$$

$$(\partial \bar{S}_e / \partial h)_{i+1}^{j+1} = [-K_e Q^2 B / (g \Delta x A^3)]_{i+1}^{j+1} \quad (14.103)$$

$$\partial L / \partial Q = 0 \quad (14.104)$$

(lateral inflow)

$$\partial L / \partial h = 0 \quad (14.105)$$

$$\partial L / \partial Q = -0.5\bar{q}/\bar{A} \quad (14.106)$$

(bulk lateral outflow)

$$\partial L / \partial h = 0.5\bar{q}\bar{Q}\bar{B}/\bar{A}^2 \quad (14.107)$$

$$\partial L / \partial Q = -0.25\bar{q}/\bar{A} \quad (14.108)$$

(seepage outflow)

$$\partial L / \partial h = 0.25\bar{q}\bar{Q}\bar{B}/\bar{A}^2 \quad (14.109)$$

In equations (14.87)–(14.94), the subscripts (l and k) denote the row and column of the element ($a_{l,k}$) within the Jacobian matrix. The subscript (l) has a value of 2 for the first Δx reach and increments by 2 for each successive Δx reach proceeding from the upstream boundary to downstream boundary. The subscript (k) has a value of 1 for the first Δx reach and increments by 2 for each successive Δx reach.

Thus, the Newton–Raphson method generates a system of $2N \times 2N$ linear equations. The Jacobian or coefficient matrix of the system is composed of the partial derivative expressions evaluated at the first estimate, X^k . The right-hand side of equation (14.83) is the residual, a vector whose values are obtained by evaluating equations (14.69) and (14.70) using the X^k estimate values for the unknown discharges and water surface elevations. Solution of the linear system described by equation (14.83) provides corrections to the first trial (estimated) values of the unknowns.

14.10.2 Matrix solution

An efficient matrix solution technique is critical to the feasibility of an implicit model. Equation (14.83) is solved by a special modification of the Gauss elimination method for solving a system of linear equations. Using matrix notation, equation (14.83) takes the following form:

$$[A]X = R \quad (14.110)$$

in which $[A]$ = the coefficient matrix with elements $a_{l,k}$ and X, R are column vectors having components x_l and r_l respectively. The coefficient matrix is banded with most of the elements being zero except for four elements in each row along the main diagonal of the matrix. An efficient solution technique was developed by Fread (1971) in which (1) the computations do not involve any of the many zero elements, thus reducing the required number of operations (addition, subtraction, division, multiplication) from $(16/3N^3 + 8N^2 + 14/3N)$ to $(38N - 19)$; and (2) stores only the non-zero elements, thus reducing the storage required for the $[A]$ matrix from $2N \times 2N$ to $2N \times 4$, where N is the total number of cross-sections along the waterway. The compaction of the original matrix into $2N \times 4$ size causes the subscript k in equations (14.87)–(14.94) not to increment for each successive Δx reach, i.e. $k = 1, 2, 3, 4$, for all l rows.

Equation (14.109) may be efficiently solved by the following compact, penta-diagonal, modified Gauss elimination algorithm. The computations to eliminate the elements below the main diagonal proceed according to $l = 2, 4, 6 \dots 2N - 2$ and are:

$$a_{l,2} = a_{l,1}/a_{l-1,k'+1} + a_{l-1,k'+2} + a_{l,2} \quad (14.111)$$

$$r_l = -a_{l,1}/a_{l-1,k'+1}r_{l-1} + r_l \quad (14.112)$$

$$a_{l+1,2} = -a_{l+1,1}/a_{l-1,k'+1}a_{l-1,k'+2} + a_{l+1,2} \quad (14.113)$$

$$r_{l+1} = -a_{l+1,1}/a_{l-1,k'+1}r_{l-1} + r_{l+1} \quad (14.114)$$

$$a_{l+1,3} = -a_{l+1,2}/a_{l,2}a_{l,3} + a_{l+1,3} \quad (14.115)$$

$$a_{l+1,4} = -a_{l+1,2}/a_{l,2}a_{l,4} + a_{l+1,4} \quad (14.116)$$

$$r_{l+1} = -a_{l+1,2}/a_{l,2}r_l + r_{l+1} \quad (14.117)$$

in which $k' = 0$ when $l = 2$ and $k' = 2$ when $l > 2$. The x_l components of the solution vector X are obtained through a back-substitution procedure commencing at $l = 2N$ and proceeding sequentially to $l = 1$. Thus,

$$x_{2N} = (-a_{2N,3}/a_{2N-1,3}r_{2N-1} + r_{2N})/(-a_{2N,3}/a_{2N-1,3}a_{2N-1,4} + a_{2N,4}) \quad (14.118)$$

$$x_l = (r_l - a_{l,k'+2}x_{l+1})/a_{l,k'+1} \quad \dots \quad l = 2N-1, 2N-3, \dots, 3, 1 \quad (14.119)$$

$$x_l = (r_l - a_{l,4}x_{l+2} - a_{l,3}x_{l+1})/a_{l,2} \quad l = 2N-2, 2N-4, \dots, 4, 2 \quad (14.120)$$

in which $k' = 2$ when $l > 1$ and $k' = 0$ when $l = 1$.

14.10.3 Enhancement of computational algorithm

FLDWAV contains an automatic procedure which increases the robust nature of the four-point, nonlinear implicit finite difference algorithm. This enhancement is quite useful when treating rapidly rising hydrographs in channels where the cross-sections have large variations in the vertical and/or along the x -axis. This situation may cause computational problems which are manifested by non-convergence in the Newton-Raphson iteration or by erroneously low computed depths at the leading edge of steep-fronted waves. When either of these manifestations are sensed, an automatic procedure consisting of two parts is implemented.

The first reduces the current time step (Δt) by a factor of 1/2 and repeats the computations. If the same problem persists, Δt is again halved and the computations repeated. This continues until a successful solution is obtained or the time step has been reduced to 1/16 of the original size. If a successful solution is obtained, the computational process proceeds to the next time level using the original Δt . If the solution using $\Delta t/16$ is unsuccessful, the θ weighting factor is increased by 0.1 and a time step of $\Delta t/2$ is used. Upon

achieving a successful solution, θ and the time step are restored to their original values. Unsuccessful solutions are treated by increasing θ and repeating the computation until $\theta = 1.0$ whereupon the automatic procedure terminates and the solution with $\theta = 1.0$ and $\Delta t/2$ is used to advance the solution forward in time now using the original θ and the Δt values. Often, computational problems can be overcome via one or two reductions in the time step.

14.11 EXTERNAL BOUNDARIES AND INITIAL CONDITIONS

External boundaries which consist of the upstream and down extremities of the waterway must be specified in order to obtain solutions to the Saint-Venant equations. In fact, in most unsteady flow applications, the unsteady disturbance is introduced to the waterway at one or both of the external boundaries.

14.11.1 Upstream boundary

Either a specified discharge or water elevation time series (hydrographs) can be used as the upstream boundary in FLDWAV. If a discharge hydrograph $Q(t)$ is used, the boundary equation is:

$$\hat{B}_1 = Q_1^{j+1} - Q(t) = 0 \quad (14.121)$$

in which case the partial derivatives for the Jacobian are:

$$a_{1,k} = \partial \hat{B}_1 / \partial Q_1 = 1 \quad (14.122)$$

$$a_{1,k+1} = \partial \hat{B}_1 / \partial h_1 = 0 \quad (14.123)$$

If a water elevation time series $h(t)$ is used, the boundary equation is:

$$\hat{B}_1 = h_1^{j+1} - h(t) = 0 \quad (14.124)$$

in which case the partial derivatives are:

$$a_{1,k} = \partial \hat{B}_1 / \partial Q_1 = \epsilon \quad (14.125)$$

$$a_{1,k+1} = \partial \hat{B}_1 / \partial h_1 = 1 \quad (14.126)$$

where ϵ is an arbitrarily small value, e.g. 0.0001. This prevents a zero value for the element $a_{1,1}$ which allows the matrix solution technique previously described to proceed without an interchange of rows needed to eliminate the zero main-diagonal element.

The hydrographs used as upstream boundary conditions should not be affected by the flow conditions downstream of the upstream boundary.

14.11.2 Downstream boundary

Specified discharge or water elevation time series may be used as the downstream boundary condition. For a discharge hydrograph $Q'(t)$, the

boundary equation is:

$$\hat{B}_N = Q_N^{j+1} - Q'(t) = 0 \quad (14.127)$$

and the partial derivatives for the Jacobian are:

$$a_{2N,k+2} = \partial \hat{B}_N / \partial Q_N = 1 \quad (14.128)$$

$$a_{2N,k+3} = \partial \hat{B}_N / \partial h_N = 0 \quad (14.129)$$

In a water elevation time series $h'(t)$ such as an observed or predicted tide, the boundary equation is;

$$\hat{B}_N = h_N^{j+1} - h'(t) = 0 \quad (14.130)$$

and

$$a_{2N,k+2} = \partial \hat{B}_N / \partial Q_N = 0 \quad (14.131)$$

$$a_{2N,k+3} = \partial \hat{B}_N / \partial h_N = 1 \quad (14.132)$$

Another frequently used downstream boundary is a relation between discharge and depth or water elevation such as a single-valued rating curve expressed in tabular (piece-wise linear) form consisting of points (Q_k, h_k) . Any discharge Q' can be obtained from the table for any associated water elevation (h_N^{j+1}) at the downstream boundary by the following linear interpolation formula:

$$Q' = Q_k + (Q_{k+1} - Q_k)(h_N^{j+1} - h_k)/(h_{k+1} - h_k) \quad (14.133)$$

In this case the downstream boundary equation is:

$$\hat{B}_N = Q_N^{j+1} - Q' = 0 \quad (14.134)$$

and

$$a_{2N,k+2} = \partial \hat{B}_N / \partial Q_N = 1 \quad (14.135)$$

$$a_{2N,k+3} = \partial \hat{B}_N / \partial h_N = -(Q_{k+1} - Q_k)/(h_{k+1} - h_k) \quad (14.136)$$

The downstream boundary can be a loop-rating curve based on the Manning equation for normal flow. The loop is produced by using the water surface slope rather than the channel bottom slope. In this case the downstream boundary equation is:

$$\hat{B}_N = Q_N^{j+1} - QN = 0 \quad (14.137)$$

where:

$$QN = 1.49 \left(\frac{A^{5/3}}{nB^{2/3}} \right)_N^{j+1} \left(\frac{h_{N-1}^j - h_N^j}{\Delta x_{N-1}} \right)^{1/2} = K_{cN} \left(\frac{h_{N-1}^j - h_N^j}{\Delta x_{N-1}} \right)^{1/2} \quad (14.138)$$

$$\text{and} \quad a_{2N,k+2} = \partial \hat{B}_N / \partial Q_N = 1 + QN/n_N^{j+1} (\Delta n / \Delta Q)_N^{j+1} \quad (14.139)$$

$$a_{2N,k+3} = \partial \hat{B}_N / \partial h_N = \frac{QN}{3} \left(3 \frac{\Delta n / \Delta h}{n} + 2 \frac{\Delta B / \Delta h}{B} - \frac{5B}{A} \right)_N^{j+1} = \frac{-QN}{K_{cN}} \frac{\Delta K_c}{\Delta h} \quad (14.140)$$

The downstream boundary can be a critical flow section; the downstream boundary equation is:

$$\hat{B}_N = Q_N^{j+1} - QC = 0 \quad (14.141)$$

$$\text{where} \quad QC = (\sqrt{g} / \bar{B} A^{3/2})_N^{j+1} \quad (14.142)$$

$$\text{and} \quad a_{2N,k+2} = \partial \hat{B}_N / \partial Q_N = 1 \quad (14.143)$$

$$a_{2N,k+3} = \partial \hat{B}_N / \partial h_N = \frac{QC}{2} \left(\frac{\Delta B / \Delta h}{B} - 3 \frac{B}{A} \right)_N^{j+1} \quad (14.144)$$

The flow at the downstream boundary should not be affected by flow conditions further downstream. Of course, there are always some minor influences on the flow due to the presence of cross-sectional irregularities downstream of the chosen boundary location; however, these usually can be neglected unless the irregularity is very pronounced such as to cause significant backwater or drawdown effects. Reservoirs or major tributaries located below the downstream boundary which cause backwater effects at the chosen boundary location should be avoided. When this situation is unavoidable, the reach of channel for which the Saint-Venant equations are being used should be extended on downstream to a location below where the tributary enters or to the dam in the case of the reservoir. Sometimes the routing reach may be shortened and the downstream boundary shifted upstream to a point where backwater effects are negligible.

14.11.3 Initial conditions

Initial conditions of water surface elevation (h) and discharge (Q) must be specified at time $t = 0$ to obtain solutions of the Saint-Venant equations. Initial conditions may be specified for FLDWAV by any of the following: (1) from observations at gauging stations with interpolated values for intermediate cross-sections; these must be sufficiently accurate to result in convergence of the Newton-Raphson solution of the Saint-Venant finite difference equations (the errors dampen-out after several time steps); (2) computed values from a previous unsteady flow solution (this is frequently used in day-to-day flood forecasting); and (3) computed values from a steady flow backwater solution.

In the case of steady flow, the discharge at all cross-sections can be

determined by:

$$Q_{i+1} = Q_i + \bar{q}_i \Delta x_i \quad \dots i = 1, 2, 3, \dots N - 1 \quad (14.145)$$

in which Q_i is the assumed steady flow at the upstream boundary at time $t = 0$, and \bar{q}_i is the known average lateral inflow (outflow) along each Δx reach at $t = 0$. The water surface elevations (h_i) are computed according to the following steady flow simplification of the momentum equation (14.62):

$$(Q^2/A)_{i+1} - (Q^2/A)_i + g\bar{A}_i(h_{i+1} - h_i + \Delta x_i \bar{S}_{f_i}) = 0 \quad (14.146)$$

in which \bar{A}_i and \bar{S}_{f_i} are defined by equations (14.71) and (14.73), respectively. The computations proceed in the upstream direction ($i = N - 1, \dots 3, 2, 1$) for subcritical flow (they proceed in the downstream direction for supercritical flow). The starting water surface elevation (h_N) can be specified or obtained from the appropriate downstream boundary condition for a discharge of Q_N . Equation (14.146) can be solved by the Newton-Raphson method as applied to a single nonlinear equation. In this case, if equations (14.83) and (14.84) are combined, the following recursive relationship can be written in scalar form;

$$x^{k+1} = x^k - f(x^k)/f'(x^k) \quad (14.147)$$

in which x represents the unknown (h_i), k is the number of iterations, $f(x^k)$ is equation (14.146) evaluated with the trial solution x^k , and $f'(x^k)$ is the derivative of equation (14.146) with respect to the unknown (h_i) and evaluated at x^k . The derivative expression follows:

$$\begin{aligned} f'(x^k) = df(x^k)/dh_i = & (Q^2 B/A^2)_i + 0.5gB_i(h_{i+1} - h_i + \bar{S}_{f_i} \Delta x_i) \\ & + g\bar{A}_i[-1 + \Delta x_i(d\bar{S}_{f_i}/dh_i)] \end{aligned} \quad (14.148)$$

in which $d\bar{S}_{f_i}/dh_i$ is defined by equation (14.96).

14.12 INTERNAL BOUNDARIES

There may be locations such as a dam, bridge, or waterfall (short rapids) along a waterway where the Saint-Venant equations are not applicable. At these locations the flow is rapidly varied rather than gradually varied as necessary for the applicability of the Saint-Venant equations. Empirical water elevation-discharge relations such as weir-flow can be utilized for simulating rapidly varying flow. In FLDWAV, unsteady flows are routed along the waterway including points of rapidly varying flow by utilizing internal boundaries. At internal boundaries, cross-sections are specified for the upstream and downstream extremities of the section of waterway where rapidly varying flow occurs. The Δx reach length between the two cross-sections can be any appropriate value from zero to the actual measured distance. Since, as with any other Δx reach, two equations (the Saint-Venant equations) are required,

the internal boundary Δx reach requires two equations. The second of the required equations represents the conservation of mass with negligible time-dependent storage, i.e.,

$$\hat{B}_{12} = Q_i^{j+1} - Q_{i+1}^{j+1} = 0 \quad (14.149)$$

and the derivatives for the Jacobian are:

$$a_{l+1,k} = \partial \hat{B}_{12} / \partial Q_i = 1 \quad (14.150)$$

$$a_{l+1,k+1} = \partial \hat{B}_{12} / \partial h_i = 0 \quad (14.151)$$

$$a_{l+1,k+2} = \partial \hat{B}_{12} / \partial Q_{i+1} = -1 \quad (14.152)$$

$$a_{l+1,k+3} = \partial \hat{B}_{12} / \partial h_{i+1} = 0 \quad (14.153)$$

The first of the two required equations is an empirical rapidly varied flow relation. Several examples of rapidly varied flow internal boundary equations follow.

14.12.1 Critical flow

If the internal boundary is used to represent critical flow, the following equation is used in conjunction with equation (14.149):

$$\hat{B}_{11} = Q_i^{j+1} - \sqrt{g}(A^{3/2}/B^{1/2})_i^{j+1} = 0 \quad (14.154)$$

and the derivatives are:

$$a_{l,k} = \partial \hat{B}_{11} / \partial Q_i = 1 \quad (14.155)$$

$$a_{l,k+1} = \partial \hat{B}_{11} / \partial h_i = 0.5\sqrt{g}[\Delta B/\Delta h(A/B)^{3/2} - 3(AB)^{1/2}]_i^{j+1} \quad (14.156)$$

14.2.2 Dam

At a dam, the internal boundary can represent any combination of flow such as spillway flow (uncontrolled overflow, fixed gate, time-dependent gate), crest overflow, constant (head-independent) flow, or breach flow due to a time-dependent failure of the dam. The general equation for flow at a dam is:

$$\hat{B}_{11} = Q_i^{j+1} - Q_d = 0 \quad (14.157)$$

where:

$$Q_d = Q_{br} + Q_s \quad (14.158)$$

in which Q_{br} is the time-dependent breach flow which may be zero and Q_s is the sum of all other types of flow. The breach flow can be expressed as broad-crested weir flow corrected for submergence effects, i.e.

$$Q_{br} = K_s Q_{br} \quad (14.159)$$

$$\text{where: } Q_{br} = 3.1b(h_i^{j+1} - h_{br})^{3/2} + 2.45z(h_i^{j+1} - h_{br})^{5/2} \quad (14.160)$$

$$K_s = 1. - 27.8(h_r - 0.67)^3 \quad \dots h_r > 0.67 \quad (14.161)$$

$$K_s = 1. \quad \dots h_r \leq 0.67 \quad (14.162)$$

$$h_r = (h_{i+1}^{j+1} - h_{br}) / (h_i^{j+1} - h_{br}) \quad (14.163)$$

$$b = \hat{b} \quad \dots t_{br} > \tau_{br} \quad (14.164)$$

$$b = \hat{b} t_{br} / \tau_{br} \quad \dots t_{br} \leq \tau_{br} \quad (14.165)$$

$$h_{br} = h_{bm} \quad \dots t_{br} > \tau_{br} \quad (14.166)$$

$$h_{br} = h_d - (h_d - h_{bm}) t_{br} / \tau_{br} \quad \dots t_{br} \leq \tau_{br} \quad (14.167)$$

in which K_s is a submergence correction factor due to the effects of the water surface elevation (h_{i+1}) downstream of the dam, b is the instantaneous width of the breach bottom, \hat{b} is the final maximum width of the breach bottom, t_{br} is the time since beginning of breach formation, τ_{br} is the interval of time necessary for the breach to completely form, h_b is the elevation of the breach bottom, h_{bm} is the final elevation of the breach bottom (usually assumed to be the bottom of the dam), h_d is the elevation of the crest of the dam, and z is the side slope of the breach (1 : vertical to z : horizontal). The values of \hat{b} , τ_{br} , h_{br} , h_d , h_{bm} , and z must be known or assumed from previous breached dams. The breach starts forming when h_i^{j+1} equals or exceeds h_f , a specified elevation representing the amount of overtopping required for failure to commence. The sum of all other flows (Q_s) is:

$$Q_s = K_{ss} Q_{ss} + Q_g + K_{cs} Q_{cs} + Q_t \quad (14.168)$$

$$Q_{ss} = c_s L_s (h_i^{j+1} - h_s)^{3/2} \quad (14.169)$$

$$Q_g = \sqrt{2g} c_g A_g (h_i^{j+1} - h_g)^{1/2} \quad (14.170)$$

$$Q_{cs} = c_d L_d (h_i^{j+1} - h_d)^{3/2} \quad (14.171)$$

$$K_{ss} = 1. - 27.8(h_{rs} - 0.67)^3 \quad \dots h_{rs} > 0.67 \quad (14.172)$$

$$h_{rs} = (h_{i+1}^{j+1} - h_s) / (h_i^{j+1} - h_s) \quad (14.173)$$

$$K_{cs} = 1. - 27.8(h_{rc} - 0.67)^3 \quad \dots h_{rc} > 0.67 \quad (14.174)$$

$$h_{rc} = (h_{i+1}^{j+1} - h_d) / (h_i^{j+1} - h_d) \quad (14.175)$$

in which K_{ss} and K_{cs} are submergence correction factors for the spillway and dam crest, respectively; c_s , c_g , and c_d are discharge coefficients for the spillway, gate(s) and dam crest, respectively; L_s is the length of the spillway; A_g is the area of the gate opening; L_d is the length of the dam crest after subtracting L_s ; h_s is the elevation of the spillway crest; h_g is the elevation of the centre of the gate(s); and Q_t is a constant, head-independent outflow. Also, time-dependent gate parameters (c_g and A_g) may be specified via tabular, piecewise linear, values and associated times (t). For further information on the expected range of the parameters in equations (14.157)–(14.175), see Fread (1980).

The partial derivatives of equation (14.157) are:

$$a_{l,k} = \partial \hat{B}_{11} / \partial Q_i = 1 \quad (14.176)$$

$$a_{l,k+1} = \partial \hat{B}_{11} / \partial h_i = -K_s \partial Q_{br} / \partial h_i - Q_{br} \partial K_s / \partial h_i - \partial Q_s / \partial h_i \quad (14.177)$$

$$\text{where: } \partial Q_{br} / \partial h_i = 4.65b(h_i^{j+1} - h_{br})^{1/2} + 6.13z(h_i^{j+1} - h_{br})^{3/2} \quad (14.178)$$

$$\partial K_s / \partial h_i = 83.4(h_r - 0.67)^2 h_r / (h_i^{j+1} - h_{br}) \quad (14.179)$$

$$\begin{aligned} \partial Q_s / \partial h_i = & 1.5K_{ss}c_sL_s(h_i^{j+1} - h_s)^{1/2} + 83.4Q_{ss}(h_{rs} - 0.67)^2 \\ & h_{rs} / (h_i^{j+1} - h_s) \\ & + 0.5\sqrt{2g}c_gA_g / (h_i^{j+1} - h_g)^{1/2} + 1.5K_{cs}c_dL_d(h_i^{j+1} - h_d)^{1/2} \\ & + 83.4Q_{cs}(h_{rc} - 0.67)^2 h_{rc} / (h_i^{j+1} - h_d) \end{aligned} \quad (14.180)$$

$$\text{and } a_{l,k+2} = \partial \hat{B}_{11} / \partial Q_{i+1} = 0 \quad (14.181)$$

$$a_{l,k+3} = \partial \hat{B}_{11} / \partial h_{i+1} = -Q_{br} \partial K_s / \partial h_{i+1} - \partial Q_s / \partial h_{i+1} \quad (14.182)$$

where:

$$\partial K_s / \partial h_{i+1} = -83.4(h_r - 0.67)^2 / (h_i^{j+1} - h_{br}) \quad (14.183)$$

$$\begin{aligned} \partial Q_s / \partial h_{i+1} = & -83.4Q_{ss}(h_{rs} - 0.67)^2 / (h_i^{j+1} - h_s) \\ & - 83.4Q_{cs}(h_{rc} - 0.67)^2 / (h_i^{j+1} - h_d) \end{aligned} \quad (14.184)$$

14.12.3 Bridge-embankment

Another internal boundary condition can be the flow occurring at a bridge and perhaps over its embankment which impedes flow in the floodplain. The total flow (Q_{be}) which may be a combination of flow through the bridge opening (Q_{bo}), flow over the embankment (Q_{em}), and flow through a time-dependent breach in the embankment (Q_{br}). The internal boundary equation for flow at a bridge embankment is:

$$\hat{B}_{i1} = Q_i^{j+1} - Q_{be} \quad (14.185)$$

$$\text{where: } Q_{be} = Q_{bo} + Q_{em} + Q_{br} \quad (14.186)$$

$$Q_{bo} = \sqrt{2g}c_b A_{i+1}^{j+1} (h_i^{j+1} - h_{i+1}^{j+1})^{1/2} \quad (14.187)$$

$$Q_{em} = K_{em} L_{em} c_{em} (h_i^{j+1} - h_{em})^{3/2} \quad (14.188)$$

$$K_{em} = 1. - 27.8(h_{re} - 0.67)^3 \quad \dots h_{re} > 0.67 \quad (14.189)$$

$$h_{re} = (h_{i+1}^{j+1} - h_e)/(h_i^{j+1} - h_{em}) \quad (14.190)$$

in which c_b is the bridge flow coefficient which accounts for piers, angle of flow approach, etc. (see Chow, 1959); c_{em} , L_{em} , K_{em} are the discharge coefficient, length of embankment, and submergence correction factor, respectively, for the embankment overflows (Fread, 1980); and the flow through a breach of the the embankment (Q_{br}) is defined as in equations (14.159)–(14.167) except h_d is replaced with h_e , the top of the embankment.

The partial derivatives of equation (14.185) are:

$$a_{l,k} = \partial \hat{B}_{l1} / \partial Q_i = 1 \quad (14.191)$$

$$\begin{aligned} a_{l,k+1} = \partial \hat{B}_{l1} / \partial h_i = & -0.5Q_{bo}/(h_i^{j+1} - h_{i+1}^{j+1}) - 1.5Q_{em}/(h_i^{j+1} - h_{em}) \\ & + 83.4Q_{em}/K_{em}(h_{re} - 0.67)^2 h_{re}/(h_i^{j+1} - h_{em}) - \partial Q_{br} / \partial h_i \end{aligned} \quad (14.192)$$

$$a_{l,k+2} = \partial \hat{B}_{l1} / \partial Q_{i+1} = 0 \quad (14.193)$$

$$\begin{aligned} a_{l,k+3} = \partial \hat{B}_{l1} / \partial h_{i+1} = & Q_{bo}[0.5/(h_i^{j+1} - h_{i+1}^{j+1}) - B_i^{j+1}/A_i^{j+1}] \\ & + 83.4Q_{em}/K_{em}(h_{re} - 0.67)^2/(h_i^{j+1} - h_{em}) - \partial Q_{br} / \partial h_{i+1} \end{aligned} \quad (14.194)$$

in which $\partial Q_{br} / \partial h_i$ is similar to the expression $K_s \partial Q_{br} / \partial h_i + Q_{br} \partial K_s / \partial h_i$ in equation (14.177) and ∂h_{i+1} is similar to the expression ($Q_{br} \partial K_s / \partial h_{i+1}$) in equation (14.182) except h_d is replaced by h_e .

14.12.4 Lock and dam

A waterway may include small dams with manually operated gates to pass the flow so as to maintain a desired depth for safe navigation upstream of the dam. A lock is provided for navigation of boats, barges, etc. past the dam. Although the actual gate operations may not be known in the application of FLDWAV, the assumed maintenance of a constant water elevation provides the internal boundary equation, i.e.

$$\hat{B}_{l1} = h_i^{j+1} - h_i = 0 \quad (14.195)$$

in which h_t is the target pool elevation which the dam operator attempts to maintain via operation of the gates. The target pool elevation may be a constant value or it may be an assumed function of time. When the computed elevation (h_{i+1}) exceeds a specified elevation, the flow is assumed then to be governed by the Saint-Venant equations.

The partial derivatives of equation (14.195) are all zero except one, i.e.

$$a_{l,k+1} = \partial B_{Tl} / \partial h_i = 1 \quad (14.196)$$

14.12.5 Rating curve

A rating curve as described previously in section 14.11 can be used as an internal boundary in which the downstream flow is assumed to have negligible effect on the flow passing the internal boundary section. The internal boundary equation is:

$$\hat{B}_{Tl} = Q_i^{j+1} - Q' = 0 \quad (14.197)$$

in which Q' is defined by equation (14.133). The partial derivatives are:

$$a_{l,k} = \partial \hat{B}_{Tl} / \partial Q_i = 1 \quad (14.198)$$

$$a_{l,k+1} = \partial \hat{B}_{Tl} / \partial h_i = -(Q_{k+1} - Q_k) / (h_{k+1} - h_k) \quad (14.199)$$

$$a_{l,k+2} = \partial \hat{B}_{Tl} / \partial Q_{i+1} = 0 \quad (14.200)$$

$$a_{l,k+3} = \partial \hat{B}_{Tl} / \partial h_{i+1} = 0 \quad (14.201)$$

14.13 CROSS-SECTIONS

14.13.1 Active flow sections

That portion of the channel cross-section in which flow occurs is termed active. In FLDWAV the active flow cross-sections may be of regular or irregular geometrical shape. Each cross-section is specified as tabular values of channel width and elevation, which together constitute a piecewise linear relationship. Experience has shown that in almost all instances the cross-section may be sufficiently described with approximately eight or less sets of widths and associated elevations. A low-flow cross-sectional area which can be zero is used to describe the cross-section below the minimum specified elevation, below which the water elevation must not recede. The total cross-sectional area below each of the widths is initially computed within the model. During the solution of the unsteady flow equations any areas or widths associated with a particular water surface elevation are linearly interpolated from the piecewise linear relationships of width and elevation which were specified or the area-elevation sets initially generated within the model.

Cross-sections at gauging station locations are generally used as computational points in the $x-t$ plane. Cross-sections are also specified at points along the river where significant cross-sectional changes occur or at points where major tributaries enter. Typically, cross-sections are spaced farther apart for large natural channels than for small channels, since the degree of variation in the cross-sectional characteristics is less for the larger channels. Spacing can range from a few hundred feet to a few miles. In addition to the consideration of cross-sectional variation in the selection of Δx reaches, the solution accuracy also affects the choice of Δx . For best accuracy, the maximum reach length (Δx_m) is related to Δt as follows:

$$\Delta x_m \leq c \Delta t \quad (14.202)$$

in which c is the wave speed of the essential characteristic of the unsteady flow such as the mid-point of the hydrograph. The wave speed may be initially estimated from equation (14.32) or from observed flows, and the time step (Δt) is selected according to equation (14.34). Since c may vary with distance along the channel, Δx_m may not be constant along the channel.

In some applications the total number of cross-sections due to geometrical variation can be reduced by using a distance-weighted average section. The width (\bar{B}) of the average section can be computed from the widths of the other sections which are to be averaged by:

$$\bar{B} = 0.5 [(B_i + B_{i+1}) \Delta d_i + (B_{i+1} + B_{i+2}) \Delta d_{i+1} + \dots + (B_{I-1} + B_I) \Delta d_{I-1}] / \sum_1^{I'} \Delta d_i \quad (14.203)$$

in which \bar{B} is the distance-weighted width for a particular depth of flow, B_i is width of the i th section along a reach having a total of (I') sections to be averaged, and Δd_i is the distance between the individual sections. The total reach length ($\sum \Delta d_i$) of equation (14.203) must be less than Δx_m of equation (14.202).

14.13.2 Off-channel storage

A cross-section may contain portions where the flow velocity in the x -direction is negligible relative to the velocity in the active portion. The inactive portion of the cross-section is known as dead or off-channel storage. Off-channel storage areas can be used to effectively account for embayments, ravines, or tributaries which connect to the flow channel but do not pass flow and serve only to store the flow. Another effective use of off-channel storage is to model a heavily wooded floodplain which stores a portion of the flood waters passing through the channel. In each of these cases the use of zero velocity for the portion of the flood waters contained in the dead storage area results in a more

realistic simulation of the actual flow than using an average velocity derived from the main flow channel and the dead storage area. The dead storage cross-sectional properties are described in the same manner as the active cross-sectional areas.

14.13.3 Linearly interpolated cross-sections

Within FLDWAV, there is an option to generate additional cross-sections between any two adjacent specified cross-sections. The properties of the additional sections are linearly interpolated. This facilitates adherence to equation (14.202) for appropriate Δx reach lengths. Both active and off-channel storage widths are generated via the interpolation procedure.

14.14 CHANNEL FRICTION

The Manning n is used to describe the resistance of flow due to channel roughness caused by bed forms, bank vegetation, obstructions, bend effects, and eddy losses. The Manning n is defined for each Δx reach as a specified function of water elevation or discharge according to a tabular (piecewise linear) relation between n and the independent variable (h or Q). Linear interpolation is used in FLDWAV to obtain n for values of h or Q intermediate to the tabular values.

Alternatively, the friction effects can be represented by channel conveyance (K_c) which may be specified in FLDWAV as a tabular function of water elevation. Conveyance is related to the Manning n and cross-sectional properties, i.e.

$$K_c = 1.49AR^{2/3}/n \quad (14.204)$$

The use of K_c rather than n has an advantage in applications where the cross-section consists of an in-bank portion and a rather wide, flat floodplain. The hydraulic radius (R) can be somewhat discontinuous when the water surface expands onto the floodplain. This discontinuity can be treated by specifying conveyance as a function of elevation which is smoothed in the vicinity of the discontinuity. This provides more realistic flows and helps to avoid numerical problems during the computations.

The channel routing computations are often sensitive to the Manning n or K_c . In the absence of necessary data (observed stages and discharges), n can be estimated; however, best results are obtained when the Manning n is adjusted to reproduce historical observations of water elevation and discharge. The adjustment process or calibration may be either trial-and-error or an automatic iterative procedure. The automatic calibration algorithm is described later.

14.15 LATERAL INFLOWS

FLDWAV incorporates small tributary inflows or overland flow via the lateral inflow term (q) in equations (14.61) and (14.62). These are considered independent of flows occurring in the river to which they are added. They are specified as a time series of flows with constant or variable time intervals. They can be specified for any Δx reach along the river as the sum of all lateral inflows within the Δx reach. Outflows may be simulated by assigning a negative sign to the specified flows. Linear interpolation is used for flows at times other than the specified intervals.

14.16 MODIFIED SAINT-VENANT EQUATIONS FOR FLOODPLAIN FLOWS

Unsteady flow in a natural river which meanders through a wide floodplain is complicated by large differences in geometric and hydraulic characteristics between the river channel and the floodplain, as well as the extreme differences in the hydraulic roughness coefficient. The flow is further complicated by the meandering of the main channel within the floodplain; this causes a portion of the total flow to 'short-circuit' and proceed downstream along the more direct course afforded by the floodplain rather than along the more circuitous route of the meandering channel. This tendency for short-circuiting of the flow is enhanced by the greater longitudinal slope associated with the floodplain than that of the main channel; however, the short-circuiting effect is diminished by the greater hydraulic roughness of the floodplain. Further complexities are created by portions of the floodplain which act as dead storage areas, wherein the flow velocity is negligible.

FLDWAV contains a modified form of the Saint-Venant equations for an alternative method for routing floods in meandering rivers with floodplains. A modification of the one-dimensional Saint-Venant equations avoids the obvious use of the more complex and computationally time-consuming two-dimensional equations. The one-dimensional equations are modified such that the flow in the meandering channel and floodplain are identified separately. Thus, the differences in both hydraulic properties and flow-path distance are taken into account in a physically meaningful way, but one that is one-dimensional in concept. This development differs from conventional one-dimensional treatment of unsteady flows in rivers with floodplains, wherein the flow is either averaged across the total cross-sectional area (channel and floodplain) or the floodplain is treated as off-channel storage and the reach lengths of the channel and floodplain are assumed to be identical.

The Saint-Venant equations are modified (Fread, 1976) as follows:

$$\frac{\partial(K_{cn}Q)}{\partial x_{cn}} + \frac{\partial(K_{lf}Q)}{\partial x_{lf}} + \frac{\partial(K_{rf}Q)}{\partial x_{rf}} + \frac{\partial(A_{cn} + A_{lf} + A_{rf} + A_0)}{\partial t} - q = 0 \quad (14.205)$$

$$\frac{\partial Q}{\partial t} + \frac{\partial(K_{cn}^2 Q^2/A_{cn})}{\partial x_{cn}} + \frac{\partial(K_{lf}^2 Q^2/A_{lf})}{\partial x_{lf}} + \frac{\partial(K_{rf}^2 Q^2/A_{rf})}{\partial x_{rf}} + gA_{cn} \left(\frac{\partial h}{\partial x_{cn}} + S_{f_{cn}} + S_e \right) + gA_{lf} \left(\frac{\partial h}{\partial x_{lf}} + S_{f_{lf}} \right) + gA_{rf} \left(\frac{\partial h}{\partial x_{rf}} + S_{f_{rf}} \right) = 0 \quad (14.206)$$

The parameters (K_{cn} , K_{lf} , K_{rf}) proportion the total flow (Q) into the channel, left floodplain, and right floodplain, respectively. These are defined as follows:

$$K_{cn} = 1/(1 + k_l + k_r) \quad (14.207)$$

$$K_{lf} = k_l/(1 + k_l + k_r) \quad (14.208)$$

$$K_{rf} = k_r/(1 + k_l + k_r) \quad (14.209)$$

and

$$k_l = \frac{Q_{lf}}{Q_{cn}} = \frac{n_{cn} A_{lf}}{n_{lf} A_{cn}} \left(\frac{R_{lf}}{R_{cn}} \right)^{2/3} \left(\frac{\Delta x_{cn}}{\Delta x_{lf}} \right)^{1/2} \quad (14.210)$$

$$k_r = \frac{Q_{rf}}{Q_{cn}} = \frac{n_{cn} A_{rf}}{n_{rf} A_{cn}} \left(\frac{R_{rf}}{R_{cn}} \right)^{2/3} \left(\frac{\Delta x_{cn}}{\Delta x_{rf}} \right)^{1/2} \quad (14.211)$$

Equations (14.210) and (14.211) represent the ratio of flow in the channel section to flow in the left and right floodplain sections; the flows are expressed in terms of the Manning equation with the energy slope approximated by the water surface slope ($\Delta h/\Delta x$). The friction slope terms in equation (14.206) are similar to equation (14.73).

Equations (14.205) and (14.206) are approximated with the weighted, four-point finite difference expressions of equations (14.66)–(14.68). The resulting finite difference equations, similar to equations (14.69) and (14.70), are solved by the Newton–Raphson iterative method for nonlinear equations using the special penta-diagonal matrix technique described by equations (14.111)–(14.120). The coefficients K_{lf} or K_{rf} are considered to be zero until the water elevation is sufficient to produce wetted top widths, B_{lf} or B_{rf} , greater than 1 ft. Thus, any terms associated with the left or right floodplain in equations (14.205) and (14.206) are set to zero, as are the derivatives associated with the terms. This avoids numerical difficulties such as division by zero, etc. during the computer solution.

14.17 SUPERCRITICAL OR MIXED FLOW

In the preceding presentation it was assumed the flow is always subcritical at each cross-section along the routing reach. When the flow becomes supercritical it requires special treatment of the external boundaries. Supercritical flow may occur all along a channel reach, or it may occur at intermittent locations along the routing reach. The former is easier to treat, while the latter ('mixed flow') is more difficult. The flow may be mixed in both time and loca-

tion along the channel. The locations of each type of flow (supercritical or subcritical) must be determined at each time step, and various types of boundary conditions must be used with each partial reach of supercritical or subcritical flow.

Supercritical flow occurs when the Froude number (F_i) is greater than that for critical flow, i.e.

$$F_i = Q_i / (\sqrt{g/B_i} A_i^{3/2}) > F_c \quad (14.212)$$

in which F_c is the Froude number for critical flow. A value of 1.0 is used for F_c , although this may be slightly changed to account for numerical effects. Subcritical flow occurs when $F_i < F_c$, and critical flow occurs when $F_i = F_c$. A *priori* estimation of the occurrence of supercritical flow is conveniently determined through use of the channel bottom slope, i.e. supercritical flow occurs if $S_0 > S_c$, where S_c (the critical slope) may be expressed as follows:

$$S_c = gn^2 / [2.21(A/B)^{1/3}] \quad (14.213)$$

14.17.1 Supercritical flow

If the entire routing reach is supercritical flow, the downstream boundary condition is no longer required since flow disturbances cannot propagate upstream; hence, the downstream boundary is superfluous. However, in order to have a determinate system of implicit difference equations, there must be $2N$ equations to match the $2N$ unknowns. The additional equation needed to make a determinate system is an additional upstream boundary equation in the form of a depth-discharge relation, i.e.,

$$\hat{B}_2 = Q_1^{j+1} - QS = 0 \quad (14.214)$$

$$\text{where: } QS = \left(\frac{1.486A^{5/3}}{nB^{2/3}} \right)_1^{j+1} \left(\frac{h_1^j - h_2^j}{\Delta x_1} \right)^{1/2} = K_{c1} \left(\frac{h_1^j - h_2^j}{\Delta x_1} \right)^{1/2} \quad (14.215)$$

The partial derivatives of equation (14.214) for the Jacobian are:

$$a_{2,1} = \partial \hat{B}_2 / \partial Q_1 = 1 \quad (14.216)$$

$$a_{2,2} = \partial \hat{B}_2 / \partial h_1 = \frac{QS}{3} \left(\frac{3}{n} \frac{dn}{dh} - \frac{5B}{A} + \frac{2}{B} \frac{dB}{dh} \right)_1^{j+1} = - \frac{QS}{K_{c1}} \frac{\Delta K_{c1}}{\Delta h_1} \quad (14.217)$$

and the subscript (l) of equations (14.87)–(14.94) starts with a value of 3 and progresses to a value of $2N - 2$ in steps of 2. The matrix solution given by equations (14.111)–(14.120) must be slightly modified since there are two upstream boundary equations and none at the downstream boundary. When determining the initial conditions, equation (14.145) can be used although the unknown is h_{i+1} and the first term for equation (14.146) becomes $(-Q^2B/A^2)_{i+1}$, B_i becomes B_{i+1} , and the -1 in the brackets becomes $+1$.

The computations proceed from upstream to downstream ($i = 1, 2, \dots, 2N - 1$); and h_i is determined by solving the Manning equation, (14.215) for h_i^{j+1} and the term $(h_1^j - h_2^j)/\Delta x_1$ is replaced with the channel bottom slope between the first and second cross sections.

14.17.2 Mixed flow

When the flow changes with either time or distance along the routing reach from supercritical to subcritical or conversely, the flow is described as 'mixed'. During each time step, subreaches are delineated where supercritical or subcritical flow exists by computing the Froude number at each cross-section and grouping consecutive Δx_i reaches into either subcritical or supercritical subreaches. Then, the Saint-Venant equations are applied and solutions obtained for each subreach, commencing with the most upstream subreach and progressing downstream until each subreach has been solved. Appropriate external boundary equations are used for each subreach.

Where the flow changes from subcritical to supercritical the downstream boundary for the subcritical subreach is the critical flow equation (14.140). The two upstream boundary equations for the supercritical subreach are:

$$\hat{B}_{r1} = Q_1^{j+1} - Q' = 0 \quad (14.218)$$

$$\hat{B}_{r2} = h_1^{j+1} - h_c = 0 \quad (14.219)$$

$$a_{1,1} = \partial \hat{B}_{r1} / \partial Q_1 = 1 \quad (14.220)$$

$$a_{1,2} = \partial \hat{B}_{r1} / \partial h_1 = 0 \quad (14.221)$$

$$a_{2,1} = \partial \hat{B}_{r2} / \partial Q_1 = 0 \quad (14.222)$$

$$a_{2,2} = \partial \hat{B}_{r2} / \partial h_1 = 1 \quad (14.223)$$

in which Q' is the computed flow at the downstream boundary of subcritical subreach, Q_1^{j+1} is the flow at the same cross-section which is now the first section of the supercritical subreach, h_c is the critical water surface elevation computed at the downstream boundary of the subcritical subreach, and h_1^{j+1} is the water elevation of the first section of the supercritical subreach. The supercritical subreach does not require a downstream boundary equation.

Where the flow changes from supercritical to subcritical, the upstream boundary equation for the subcritical subreach is:

$$\hat{B}_{r1} = Q_1^{j+1} - Q'' = 0 \quad (14.224)$$

in which Q'' is the computed flow at the last cross-section of the supercritical reach and Q_1^{j+1} is the flow at the first cross-section of the subcritical subreach. The downstream boundary for the subcritical subreach would be equation

(14.140) if another supercritical subreach exists below the subcritical subreach or the appropriate condition described by equations (14.126)–(14.140) if the subcritical subreach is the last subreach in the routing reach. The depth of flow at the first section of the subcritical subreach is determined by the downstream boundary condition and the Saint-Venant equations applied to the subcritical subreach. A hydraulic jump occurs between the last section of the supercritical subreach and the first section of subcritical subreach, although an equation for such is not directly used. To account for the possible movement of the hydraulic jump, the following procedure is utilized before advancing to the next time step: (1) the water elevation at the first section of the subcritical subreach is extrapolated to several upstream cross-sections near the downstream end of the supercritical subreach; (2) the sequent depths (water elevations) of the same sections in the supercritical reach are computed; and (3) the sequent elevations are compared with the extrapolated elevations, and the first section of the subcritical subreach is determined as that section nearest the intersection of two elevations.

14.18 THE CHANNEL NETWORKS

The implicit formulation of the Saint-Venant equations is well-suited from the standpoint of accuracy for simulating unsteady flows in a network of channels since the response of the system as a whole is determined within a certain convergence criterion for each time step. However, a network of channels presents complications in achieving computational efficiency when using the implicit formulation. Equations representing the conservation of mass and momentum at the confluence of two channels produce a Jacobian matrix in the Newton–Raphson method with elements which are not contained within the narrow band along the main diagonal of the matrix. The column location of the elements within the Jacobian depends on the sequence numbers of the adjacent cross-sections at the confluence. The generation of such ‘off-diagonal’ elements produces a ‘sparse’ matrix containing relatively few non-zero elements. Unless special matrix solution techniques are used for the sparse matrix, the computation time required to solve the matrix by conventional matrix solution techniques is so great as to make the implicit method unfeasible. The same situation also occurs for the linearized implicit methods which must also solve a system of linear equations similar to the Jacobian. One of two algorithms can be selected in FLDWAV for an efficient computational treatment of channel networks.

The first, called the ‘relaxation’ algorithm, is restricted to a dendritic (tree-type) network of channels in which the main channel has any number of tributary channels joining with it. Sometimes, dendritic systems with second-order tributaries (tributaries of tributaries) can be accommodated in the relaxation technique by reordering the dendritic system, i.e. selecting another

branch of the system as the main channel. In the relaxation algorithm no sparse matrix is generated; the Jacobian is always banded as it is for a single channel reach.

The second, called the 'network' algorithm, can be used on almost any natural system of channels (dendritic systems having any order of tributaries; bifurcating channels such as those associated with islands, deltas, flow bypasses between parallel channels; and tributaries joining bifurcated channels). The network algorithm produces a sparse matrix which is solved by a special matrix technique which is described later. The relaxation algorithm is slightly more efficient than the network algorithm, but the former does not have the versatility of the latter.

14.18.1 Relaxation algorithm

During a time step the relaxation algorithm solves the Saint-Venant equations first for the main channel and then separately for each tributary of the first-order dendritic network. The tributary flow at each confluence with the main channel is treated as lateral flow (q) which is first estimated when solving Saint-Venant equations for the main channel. Each tributary flow depends on its upstream boundary condition, lateral inflows along its reach, and the water surface elevation at the confluence (downstream boundary for the tributary) which is obtained during the simulation of the main channel. Due to the interdependence of the flows in the main channel and its tributaries, the following iterative or relaxation algorithm (Fread, 1973) is used:

$$q^* = \alpha q + (1 - \alpha)q^{**} \quad (14.225)$$

in which α is a weighting factor ($0 < \alpha \leq 1$), q is the computed tributary flow at each confluence, q^{**} is the previous estimate of q , and q^* is the new estimate of q . Convergence is attained when q is sufficiently close to q^{**} , i.e. $|q - q^{**}| < \epsilon_Q$. Usually, one or two iterations is sufficient; however, the weighting factor has an important influence on the algorithm's efficiency. Optimal values of α can reduce the iterations by as much as half. *A priori* selection of α is difficult since it varies with each dendritic system. Good first approximations for α are in the range $0.6 \leq \alpha \leq 0.8$.

The acute angle (ω_t) that the tributary makes with the main channel is a specified parameter. This enables the inclusion of the momentum effect of the tributary inflow via the term ($-qv_x$) of equation (14.80) as used in the momentum equation, equation (14.62). The velocity of the tributary inflow is given by:

$$V_x = (Q/A)_N \cos \omega_t \quad (14.226)$$

in which N denotes the last cross-section of the tributary.

14.18.2 Network algorithm

The network algorithm is used when the channel network consists of any or all of the following: (1) second- and higher-order tributaries; (2) bifurcations around islands with either zero, one, or two bypasses through the island; (3) dendritic branches joining any portion of the bifurcated branches; and (4) a dendritic network associated with river delta formations. The algorithm is based on the treatment of the channel junctions (confluences, bifurcations) as internal boundary conditions using the following three equations:

$$\hat{B}_{R1} = Q_i^{j+1} + Q_{i'}^{j+1} - Q_{i'+1}^{j+1} - \Delta s / \Delta t^j = 0 \quad (14.227)$$

$$\hat{B}_{R2} = 2g(h_i^{j+1} - h_{i'+1}^{j+1}) + (Q^2/A^2)_i^{j+1} - \Upsilon(Q^2/A^2)_{i'+1}^{j+1} = 0 \quad (14.228)$$

$$\hat{B}_{R3} = 2g(h_{i'}^{j+1} - h_{i'+1}^{j+1}) + (Q^2/A^2)_{i'}^{j+1} - \Upsilon(Q^2/A^2)_{i'+1}^{j+1} = 0 \quad (14.229)$$

where: $\frac{\Delta s}{\Delta t} = \Delta x_i / (6 \Delta t^j) \bar{B}(h_i^{j+1} + h_{i'}^{j+1} + h_{i'+1}^{j+1} - h_i^j - h_{i'}^j - h_{i'+1}^j)$ (14.230)

$$i' = i + m + 1 \quad (14.231)$$

$$\bar{B} = B_i^j + B_{i'+1}^j + B_{i'}^j \cos \omega_r \quad (14.232)$$

$$\Upsilon = 1 + C_m + C_f \quad (14.233)$$

$$C_m = (0.1 + 0.83 Q_{i'}^j / Q_{i'+1}^j) (\omega_r / 90)^\mu \quad (14.234)$$

$$C_f = 2g \Delta x_i \bar{n}^2 / [2.21 (\bar{D}^{4/3})^j] \quad (14.235)$$

in which \bar{D} is the average depth in the junction, \bar{n} is the Manning n for the junction, ω_r is the acute angle between the upstream reach and the branch, μ is an exponent taken as unity, and m is the total number of Δx reaches located upstream (downstream) along the branching channel. The parameters C_m and C_f are related to the head loss due to mixing (Lin and Soong, 1979) and friction effects, respectively. They can be specified as zero values in FLDWAV.

The partial derivatives of equation (14.227) for the Jacobian are:

$$a_{i,l-1} = \partial \hat{B}_{R1} / \partial Q_i = 1 \quad (14.236)$$

$$a_{i,l} = \partial \hat{B}_{R1} / \partial h_i = -\bar{B} \Delta x_i / (6 \Delta t^j) \quad (14.237)$$

$$a_{i,l+k} = \partial \hat{B}_{R1} / \partial Q_{i'} = 1 \quad (14.238)$$

$$a_{i,l+k+1} = \partial \hat{B}_{R1} / \partial h_{i'} = -\bar{B} \Delta x_i / (6 \Delta t^j) \quad (14.239)$$

$$a_{i,l+k+2} = \partial \hat{B}_{R1} / \partial Q_{i'+1} = -1 \quad (14.240)$$

$$a_{i,l+k+3} = \partial \hat{B}_{R1} / \partial h_{i'+1} = -\bar{B} \Delta x_i / (6 \Delta t^j) \quad (14.241)$$

The derivatives of equation (14.228) are:

$$a_{l', l' - k'} = \partial \hat{B}_{R2} / \partial Q_i = 2(Q/A^2)^{i+1} \quad (14.242)$$

$$a_{l', l' - k' + 1} = \partial \hat{B}_{R2} / \partial h_i = 2g - 2(Q^2 B/A^3)^{i+1} \quad (14.243)$$

$$a_{l', l' - 1} = \partial \hat{B}_{R2} / \partial Q_{i+1} = 2\Upsilon(Q/A^2)^{i+1} \quad (14.244)$$

$$a_{l', l'} = \partial \tilde{B}_{R2} / \partial h_{i+1} = -2g - 2\Upsilon(Q^2 B/A^3)^{i+1} \quad (14.245)$$

The partial derivatives of equation (14.229) are;

$$a_{l'+1, l' - 1} = \partial \hat{B}_{R3} / \partial Q_i = 2(Q/A^2)^{i+1} \quad (14.246)$$

$$a_{l'+1, l'} = \partial \hat{B}_{R3} / \partial h_i = 2g - 2(Q^2 B/A^3)^{i+1} \quad (14.247)$$

$$a_{l'+1, l'+1} = \partial \hat{B}_{R3} / \partial Q_{i+1} = -2\Upsilon(Q/A^2)^{i+1} \quad (14.248)$$

$$a_{l'+1, l'+2} = \partial \hat{B}_{R3} / \partial h_{i+1} = -2g + 2\Upsilon(Q^2 B/A^3)^{i+1} \quad (14.249)$$

The subscript (l) is determined by the sequence number of the most upstream cross-section. The subscripts (l' , k' , k'') are automatically determined so as to minimize the number of off-diagonal elements in the Jacobian and to minimize the creation of new off-diagonal elements during the elimination phase of the matrix solution. Also, the way in which the cross-sections are assigned sequential numbers within the channel network is most important in effecting the desired minimization. The numbering scheme is as follows: numbers run consecutively in the downstream direction until a dendritic-type junction is reached; then the most upstream section of the dendritic branch is given the next consecutive number and the numbers increase in the downstream direction along this branch until another junction is reached; then the most upstream section of that dendritic branch is numbered and the numbers increase in the downstream direction along that branch until a new junction is reached; this is repeated until all sections have been numbered, including the first cross-section of the branch of the very first dendritic-type junction; then the numbers continue to increase along the downstream branch of this junction. Bifurcations are numbered in a similar manner.

Computational efficiency is achieved by use of a specially developed matrix solution technique of the Gauss elimination type which operates on only non-zero elements in the matrix through use of a specified code number for each cross-section in the network of channels. The specified code number is as follows: (1) regular cross-section, (2) upstream boundary, (3) downstream boundary, (4) dendritic-type junction, (5) dendritic-type junction emanating from a bifurcated channel branch, (6) upstream junction of a bifurcation around an island, (7) downstream junction of a bifurcation around an island, (8) bifurcation-type junction emanating from another bifurcated channel and joining with a third bifurcated channel, and (9) bifurcation-type junction

emanating from a bifurcated channel and joining into the other branch of the bifurcated channel.

Three subroutines in the FLDWAV program accomplish the special treatment of channel networks. The first determines the appropriate row and column numbers of the derivative elements in the Jacobian, the second evaluates the derivatives, and the third solves the matrix. The Jacobian is a $2N \times 2N$ matrix. The number of operations (addition, subtraction, multiplication, division) required to solve the matrix is approximately $(102 + 46J)N$, where J is the total number of junctions. This is compared with $(95N - 48)$ operations for the relaxation algorithm, $(38N - 19)$ for a single channel using equations (14.111)–(14.119), and $16/3N^3 + 8N^2 + 14/3N$ for a standard Gauss elimination method for solving a $2N \times 2N$ matrix. Generally, the simulation of a channel network requires about two to three times as much computational effort as a single channel when each have N cross-sections.

14.19 LEVEE EFFECTS

Flows which overtop a levee located along either side or both sides of a channel may be simulated in FLDWAV, since any number of Δx reaches may bypass flow via a broadcrested weir-flow equation to another channel which represents the floodplain (beyond the levee). If the system of channels including floodplain channels is treated by the relaxation technique, the floodplain channel may either directly connect back into the waterway at some downstream location, or it may be disconnected as in the case of the floodplain within a ringed levee where the flow is ponded with no exit. If the channel system is treated by the network technique, the floodplain must hydraulically connect with the waterway. The hydraulic connection may be either a natural confluence or a flap-gated gravity drainage pipe. The flow in the floodplain can affect the overtopping levee flows via a submergence correction factor K_{ie} similar to that used at internal boundaries of dams. The flow may also pass from the waterway to the floodplain through a time-dependent crevasse (breach) in the levee using a breach-flow equation similar to that used at internal boundaries of dams.

The overtopping and/or breach flow is routed through the floodplain which is considered to be a tributary of the waterway along which the levee is located. The tributary (floodplain) channel must have a fictitious low-flow channel in which a small steady flow occurs at all times before the lateral inflow from the overtopped (breached) levee enters. The low flow which is specified via the upstream boundary condition for the tributary is necessary so that the Saint-Venant equations applied to the tributary can be continuously solved during the simulation; however, at the hydraulic connection with the channel, the fictitious low flow is not added to the channel flow, nor is it included in the flow that ponds within a ringed levee.

Depending on the relative elevations in the channel and floodplain (tributary), the overtopping levee flow can reverse its direction and flow from the floodplain back into the channel. Each Δx_i reach for the channel has a corresponding Δx_m reach along the floodplain channel. Each Δx_i reach has a submergence correction factor (K_{le}), a broadcrested weir flow coefficient (C_{le}), and a mean elevation (h_{le}) of the top of the levee. The effect of the levee flow is achieved by considering it to be lateral inflow or outflow (q) in equations (14.61) and (14.62). When routing the flow in the channel, if the flow overtops the levee and enters the floodplain it is considered to be bulk lateral outflow. When routing the flow in the floodplain the levee overtopping flow is considered to be lateral inflow. In either case the overtopping flow is computed as follows:

$$q_{le_i} = S_g C_{le_i} K_{le_i} (\hat{h} - h_{le_i})^{3/2} \quad \dots \hat{h} > h_{le_i} \quad (14.250)$$

where
$$S_g = (\hat{h} - \tilde{h}) / |\hat{h} - \tilde{h}| \quad (14.251)$$

$$\hat{h} = \bar{h}_i \quad \dots \bar{h}_i > h_{tm} \quad (14.252)$$

$$\hat{h} = \bar{h}_{tm} \quad \dots \bar{h}_i < h_{tm} \quad (14.253)$$

$$\tilde{h} = \bar{h}_{tm} \quad \dots \bar{h} > h_{tm} \quad (14.254)$$

$$\tilde{h} = \bar{h}_i \quad \dots \bar{h}_i < h_{tm} \quad (14.255)$$

$$\bar{h}_i = 0.5(h_i^{j+1} + h_i^{j+1}) \quad (14.256)$$

$$\bar{h}_{tm} = 0.5(h_{tm}^{j+1} + h_{tm}^{j+1}) \quad (14.257)$$

$$K_{le_i} = 1 \quad \dots \gamma \leq 0.67 \quad (14.258)$$

$$K_{le_i} = 1. - 27.8(\gamma - 0.67)^3 \quad \dots \gamma > 0.67 \quad (14.259)$$

$$\gamma = (\tilde{h} - h_{le_i})(\hat{h} - h_{le_i}) \quad (14.260)$$

in which S_g determines the appropriate sign (– for outflow, + for inflow), \bar{h}_i is the average water elevation along the Δx_i reach, h_{tm} is the average water elevation along the same Δx reach of the floodplain. Of course, the lateral flow may be zero when the water elevation in either channel does not overtop the levee or when the elevations are exactly the same, i.e.

$$q_{le_i} = 0 \quad \dots \hat{h} < h_{le_i}, \tilde{h} < h_{le_i} \quad (14.261)$$

$$q_{le_i} = 0 \quad \dots \hat{h} = \tilde{h} \quad (14.262)$$

Additional terms must be included in certain elements of the Jacobian in the Newton–Raphson solution to account for the effect of the levee lateral inflow (outflow). In equation (14.88) the following additional term is required:

$$-\theta \Delta x_i \partial q / \partial h_i = -\theta \Delta x_i q_{le_i} \left[\frac{1.5 \partial \bar{h} / \partial h_i}{(\bar{h} - h_{le_i})} - \frac{83.4(\gamma - 0.67)^2 \partial \gamma / \partial h_i}{K_{le_i}} \right] \quad (14.263)$$

$$\text{where:} \quad \partial \bar{h} / \partial h_i = 0.5 \quad \dots \quad \bar{h}_i > \bar{h}_{i_m} \quad (14.264)$$

$$\partial \bar{h} / \partial h_i = 0 \quad \dots \quad \bar{h}_i \leq \bar{h}_{i_m} \quad (14.265)$$

$$\partial \gamma / \partial h_i = -0.5\gamma / (\bar{h} - h_{le_i}) \quad \dots \quad \bar{h}_i > \bar{h}_{i_m}, \gamma > 0.67 \quad (14.266)$$

$$\partial \gamma / \partial h_i = 0.5 / (\bar{h} - h_{le_i}) \quad \dots \quad \bar{h}_i < \bar{h}_{i_m}, \gamma > 0.67 \quad (14.267)$$

In equation (14.90) the additional term is $\partial q / \partial h_{i+1}$ which is given by the same expression as in equation (14.263) except h_i is replaced with h_{i+1} . When applying the Saint-Venant equations to the Δx_m reach of floodplain, equation (14.263) is used to introduce the additional terms in equations (14.88) and (14.90). However, in this case the expression in equations (14.243)–(14.267) must be slightly modified, i.e. \hat{h} , \bar{h} and h_i are replaced with \bar{h}_i , \tilde{h}_i h_{i_m} , respectively.

The overtopping levee flow is assumed to enter perpendicular to the direction of flow in the floodplain. Thus, the lateral flow does not affect the conservation of momentum equation (14.62) except when it is considered to be bulk lateral outflow. In this case, equations (14.106) and (14.107) are appropriate.

14.20 MODEL CALIBRATION (AUTOMATIC)

Calibration is the process by which values of model parameters are adjusted until results of simulations correspond to measured (observed) flow conditions. A critical task in the calibration of dynamic wave models such as FLDWAV is the determination of the Manning n which often varies with discharge or stage, and with distance along the waterway. Calibration may be a manual trial-and-error process; however, FLDWAV has an option to automatically determine the optimum Manning n which will minimize the difference between computed and observed hydrographs via a highly efficient optimization technique (Fread and Smith, 1978). The technique can be applied to a single reach of waterway or any dendritic system which can be simulated with the relaxation method. The Manning n or conveyance factor (K_c) may be constant or have a piecewise linear variation with either discharge or water elevation for each reach of the waterway bounded by gauging stations from which observed water elevation hydrographs are available.

In the automatic calibration technique optimum Manning n values are sequentially determined for each reach bounded by gauging stations, commencing with the most upstream reach and progressing reach-by-reach in the downstream direction. Dendritic river systems are decomposed into a series of

single reaches connected by appropriate external boundary conditions. Tributaries are calibrated before the main-stem waterway and their flows are added to the main stem as lateral inflows. An observed discharge hydrograph is specified at the upstream boundary of each waterway, while an observed water elevation hydrograph at the downstream gauging station of each reach is used as the downstream boundary condition. The computed water elevation hydrograph at the upstream boundary is tested against the observed hydrograph at that point. Statistics of bias (Φ_j) and root-mean-square (r.m.s.) error are computed for $j = 1, 2, 3, \dots, J$ ranges of discharge or water elevation so that the Manning n or K_c can be calibrated as a function of discharge or stage. For each range of discharge, an improved estimate of the optimum Manning n (n_j^{k+1}) is obtained via a modified Newton-Raphson iterative method, i.e.

$$n_j^{k+1} = n_j^k - \frac{\Phi_j^k (n_j^k - n_j^{k-1})}{(\Phi_j^k - \Phi_j^{k-1})} \quad \dots k > 2; j = 1, 2, \dots, J \quad (14.268)$$

in which the k superscript denotes the number of iterations and Φ_j is the bias for the j th range. Equation (14.268) can be applied only for the second and successive iterations; therefore, the first iteration is made using the following estimator:

$$n_j^{k+1} = n_j^k (1.0 - 0.01 \Phi_j^k / |\Phi_j^k|) \quad \dots k = 1; j = 1, 2, \dots, J \quad (14.269)$$

in which a small percentage change in the Manning n is made in the correct direction as determined by the term $(-\Phi_j^k / |\Phi_j^k|)$. The convergence properties of equation (14.268) are quadratic with convergence usually obtained within three to five iterations. Improved Manning n values obtained via equation (14.268) are used and the cycle repeated until a minimum r.m.s. error for the reach is found. Then, the discharges computed at the downstream boundary using the optimum Manning n are stored internally and specified as the upstream boundary condition for the next downstream reach.

Computational requirements for the calibration technique are less than twice that required for an application of FLDWAV to the same waterway without the calibration option utilized.

14.21 SELECTED APPLICATIONS OF FLDWAV

Four applications of FLDWAV are presented. They include: (1) a long, very mild sloping large river with a slow rising flood wave; (2) a dendritic river system consisting of four mild sloping large rivers with moderately rising flood waves and mutual backwater effects among the channels of the network; (3) a large, very mild sloping dendritic river system affected by a large tide at its mouth; and (4) a moderately sloping river subjected to a rapidly rising dam-break flood wave. These applications represent a wide spectrum of wave and

channel characteristics for which the dynamic wave model is particularly well-suited and potentially the most accurate of the routing models.

14.21.1 Lower Mississippi

FLDWAV was applied to a 291.7 mile reach of the Lower Mississippi River from Red River Landing to Venice shown schematically in Figure 14.2. Six intermediate gauging stations at Baton Rouge, Donaldsonville, Reserve, Carrollton, Chalmette, and Point a la Hache were used to evaluate the simulations. This reach of the Lower Mississippi is contained within levees for most of its length, although some overbank flow occurs along portions of the upper 70 miles. Throughout the reach the alluvial river meanders between deep bends and relatively shallow crossings; the sinuosity coefficient is 1.6. The low flow depth varies from a minimum of 30 ft at some crossings to a maximum depth of almost 200 ft in some bends. The average channel width is approximately $\frac{1}{2}$ mile. The average channel bottom slope is a very mild, 0.000064. The Manning n varies from about 0.012 to 0.030. The discharge varies from low flows of about 100,000 cfs to flood discharges of over 1,200,000 cfs. A total of 25 cross-sections located at unequal intervals ranging from 5 to 20 miles were used to describe the 291.7 mile reach.

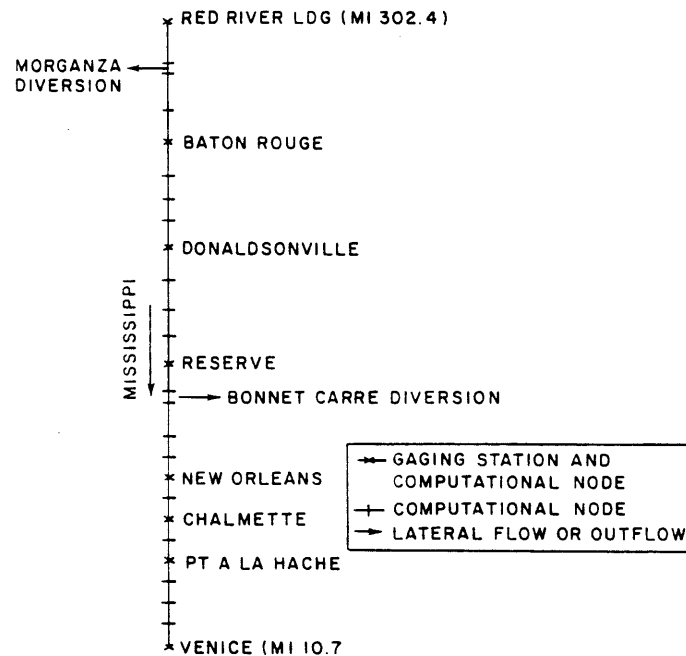


Figure 14.2 Schematic of Lower Mississippi River

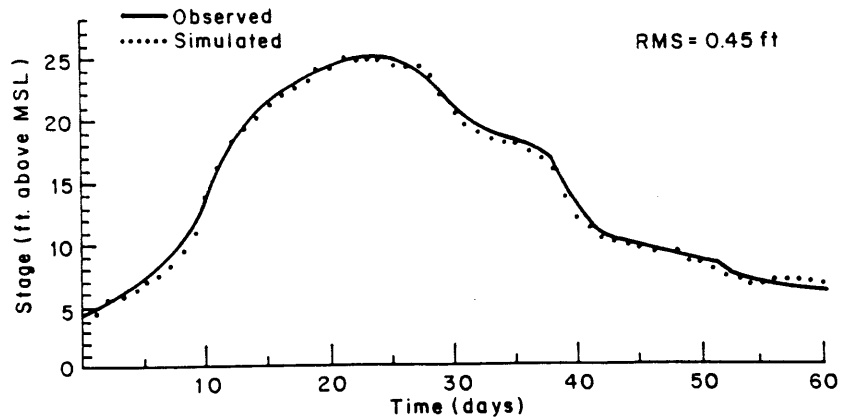


Figure 14.3 Observed vs. simulated stages at Donaldsonville for 1966 flood

The reach was first automatically calibrated by FLDWAV for the 1969 spring flood. Time steps of 24 hours were used. Then, using the calibrated set of Manning n vs. discharge for each reach bounded by gauging stations, the 1969 flood was simulated using water elevation (stage) hydrographs for upstream and downstream boundaries at Red River Landing and Venice, respectively. The simulated stage hydrographs at the six intermediate gauging stations were compared with the observed hydrographs. The r.m.s. error was used as a statistical measure of the accuracy of the calibration. The r.m.s. error varied from 0.17 to 0.36 ft with an average value of 0.25 ft.

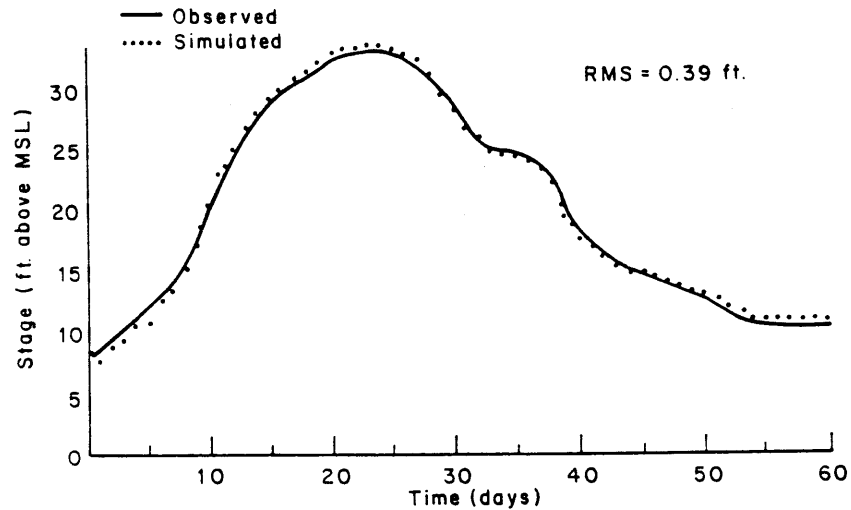


Figure 14.4 Observed vs. simulated stages at Baton Rouge for 1966 flood

Table 14.1 Summary of flood simulations in Lower Mississippi River (Red River Landing to Venice) for the years 1959–1971

Year	Average r.m.s. error (ft.)	Peak discharge (1000 cfs)
1959	0.62	750
1960	0.31	850
1961	0.47	1220
1962	0.61	1155
1963	0.38	905
1964	0.51	1140
1965	0.44	1040
1966	0.38	1090
1967	0.38	700
1968	0.36	980
1969*	0.25	1065
1970	0.91	1080
1971	0.46	940

*Calibrated

Several historical floods from the period 1959–71 were then simulated using the calibrated Manning n values obtained from the 1969 flood. An example of simulated vs. observed stages is shown in Figures 14.3 and 14.4 for the 1966 flood. Average r.m.s. errors for all six stations for each of the simulated floods are shown in Table 14.1. The average r.m.s. error for all the floods was 0.47 ft. This compares with 0.25 ft for the calibrated flood of 1969, indicating that for this reach of the Mississippi there is not a significant change in the channel roughness from one flood event to another. A calibration run required 7 s on an IBM 360/195 computer system while a normal simulation run required 6 s.

14.21.2 Mississippi–Ohio–Cumberland–Tennessee System

A dendritic channel system consisting of 393 miles of the Mississippi–Ohio–Cumberland–Tennessee (MOCT) River System was also simulated using FLDWAV. A schematic of the river system is shown in Figure 14.5. Eleven intermediate gauging stations located at Fords Ferry, Golconda, Paducah, Metropolis, Grand Chain, Cairo, New Madrid, Red Rock, Grand Tower, Cape Girardeau, and Price Landing were used to evaluate the simulation.

In applying FLDWAV to this system the main channel was considered to be the Ohio–Lower Mississippi segment with the Cumberland, Tennessee, and Upper Mississippi considered as first-order tributaries. The channel bottom slope is mild, varying from about 0.000047 to 0.000095. Each branch of the river system is influenced by backwater from downstream branches. Total discharge through the system varies from low flows of approximately

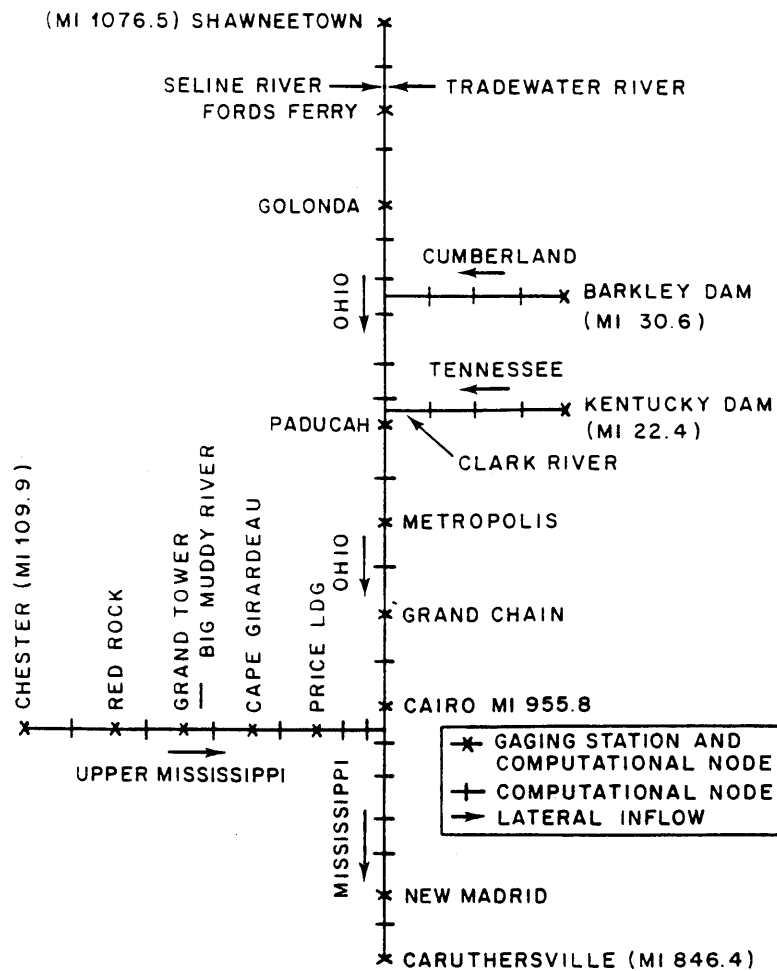


Figure 14.5 Schematic of Mississippi-Ohio-Cumberland-Tennessee (MOCT) River System

120,000 cfs to flood flows of 1,700,000 cfs. A total of 45 cross-sections located at unequal intervals ranging from 0.5 to 20 miles were used to describe the MOCT river system.

The MOCT system was calibrated to determine the $n-Q$ relationship for each of 15 reaches bounded by gauging stations. Time steps of 24 h were used. About 25 s of IBM 360/195 CPU time were required by FLDWAV to perform the calibration; a simulation run required only about 15 s. The flood of 1970 was used in the automatic calibration process. The average r.m.s. error for all 15 reaches was 0.60 ft. Typical comparisons of observed and simulated stages

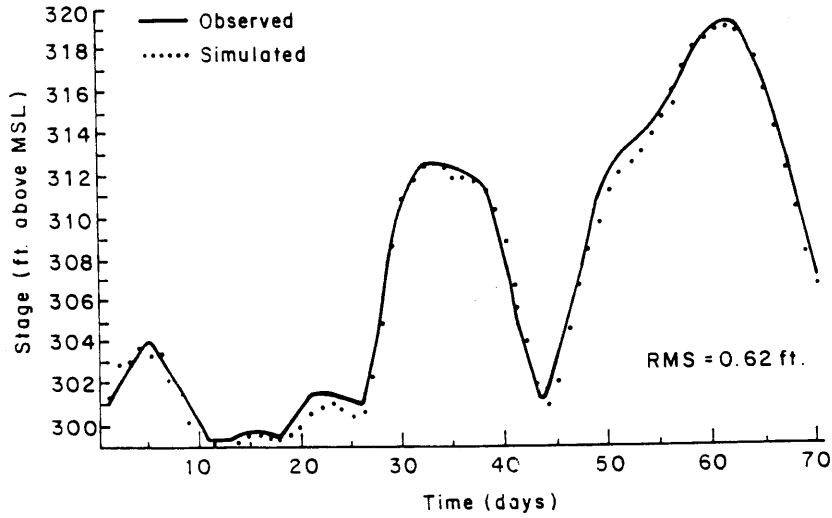


Figure 14.6 Observed vs. simulated stages at Cairo for 1970 flood

for the Cairo and Cape Girardeau gauging stations are shown in Figures 14.6 and 14.7 respectively.

Using the calibrated $n-Q$ relations, the 1969 flood was simulated. Stage hydrographs at Shawneetown and Chester and discharge hydrographs at

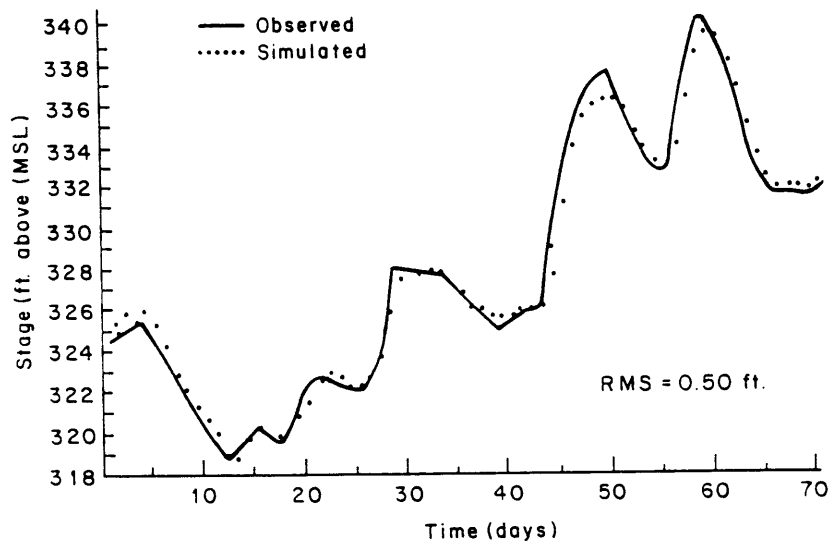


Figure 14.7 Observed vs. simulated stages at Cape Girardeau for 1970 flood

Barkely Dam and Kentucky Dam were used as upstream boundary conditions, and a rating curve was used as the downstream boundary condition at Caruthersville. The average r.m.s. error for the 11 intermediate gauging stations was 0.56 ft.

14.21.3 Columbia-Willamette System

FLDWAV was applied to the 130-mile reach of the lower Columbia River below Bonneville Dam, including the 25-mile tributary reach of the lower Willamette River. A schematic of the river system is shown in Figure 14.8.

This reach of the Columbia has a very flat slope (0.000011) and the flows are affected by the tide from the Pacific Ocean. The tidal effect extends as far upstream as the tailwater of Bonneville Dam during periods of low flow. Reversals in discharge during low flow are possible as far upstream as Vancouver. A total of 25 cross-sections located at unequal distance intervals ranging from 0.6 to 12 miles were used to describe the river system. One-hour time steps were used in the simulations which required about 11 s on an IBM 360/5 computer system.

The system was first calibrated for a 4-day period in August 1973. Seven

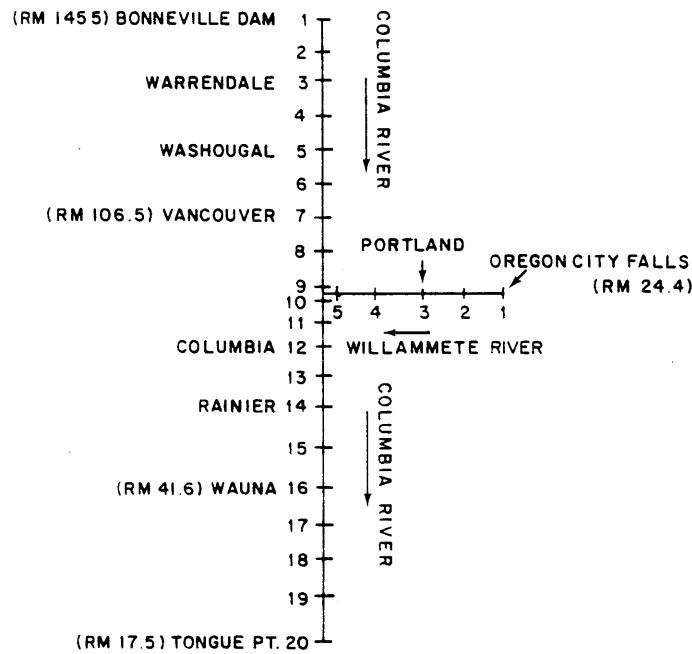


Figure 14.8 Schematic of lower Columbia-Willamette River System

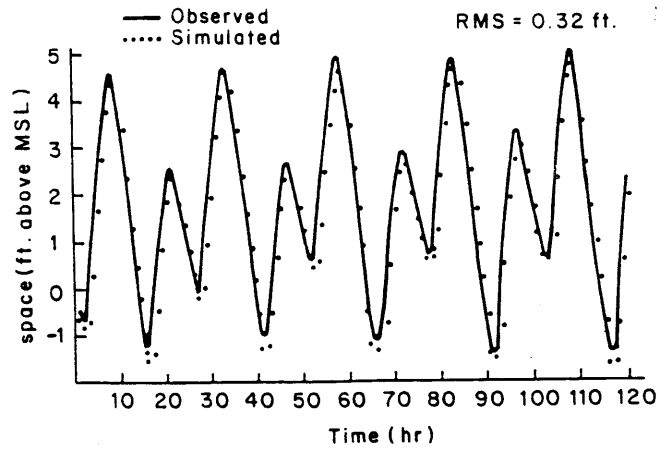


Figure 14.9 Observed vs. simulated stages at Wauna

intermediate gauging stations at Warrendale, Washougal, Vancouver, Portland, Columbia City, Rainier, and Wauna were used along with the gauging stations at the extremities of the system, i.e., Bonneville, Oregon Falls, and Tongue Point. Another 5-day period in August 1973 was then simulated using the calibrated $n-Q$ relations. Upstream and downstream boundaries were observed discharges and stages, respectively. The average r.m.s. error for all stations in the simulation run was 0.21 ft. Some examples of simulated and observed stage hydrographs for Portland and Wauna are shown in Figures 14.9 and 14.10, respectively.

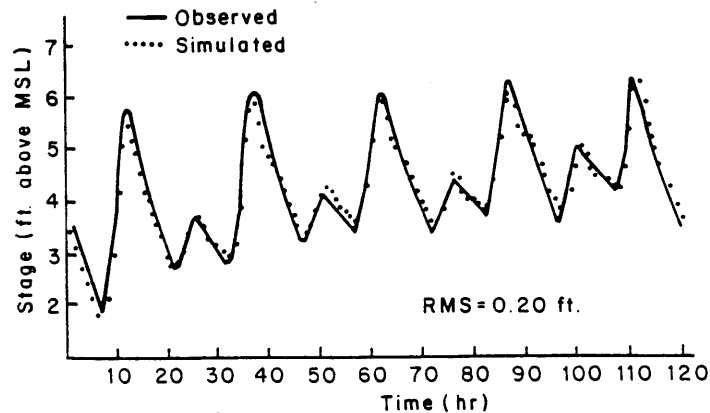


Figure 14.10 Observed vs. simulated stages at Portland

14.21.4 Teton Dam-break flood

The Teton Dam, a 300-ft high earthen dam with a 3000-ft long crest, failed on 5 June 1976, killing 11 people, making 25,000 people homeless, and inflicting about \$400 million in damages to the downstream Teton-Snake River Valley. Data from the US Geological Survey provided observations on the approximate development of the breach, description of the reservoir storage, downstream cross-sections and estimate values of the Manning's n approximately every 5 miles, indirect peak discharge measurement at three sites, flood peak travel times, and flood peak elevations. The inundated area is shown in Figure 14.11.

The following breach parameters were used in DAMBRK to reconstitute the downstream flooding due to the failure of Teton Dam: $\tau_{br} = 1.25$ h, $\delta = 150$ ft, $z = 0$, $h_{bm} = 0.0$, $h_f = h_d = 261.5$ ft, $Q = 16,000$ cfs. The initial depth of the reservoir was 261.5 ft. Cross-sections at 12 locations shown in Figure 14.11 along the 60-mile reach of the Teton-Snake River Valley below the dam were used. The average bottom slope of the 60-mile reach is 0.00135. Five top widths were used to describe each cross-section. The downstream valley consists of a narrow canyon (approximately 1000 ft wide) for the first 5 miles and thereafter a wide valley which was inundated to a width of about 9 miles. The estimated Manning n values vary from 0.028 to 0.047. Additional cross-sections were interpolated such that computational reach lengths varied from 0.5 to 1.5 miles. The downstream boundary was assumed to be channel flow control as represented by a loop rating curve giving by equation (14.136).

The computed outflow hydrograph is shown in Figure 14.11. It has a peak value of 1,652,300 cfs, a time to peak of 1.25 h, and a total duration of about 6 h. The peak is about 20 times greater than the flood of record. The temporal variation of the computed outflow volume compared within 5 per cent of observed values. The computed peak discharge values along the 60-mile downstream valley are shown in Figure 14.12 along with three observed (indirect measurement) values at miles 8.5, 43.0, and 59.5. The average difference between the computed and observed values is 4.8 per cent. Most apparent is the extreme attenuation of the peak discharge as the flood wave propagates through the valley. Losses due to infiltration and detention storage behind irrigation levees were assumed to vary from zero to a maximum of -0.30 cfs/ft and were accounted for by the lateral outflow (q) in equation (14.61).

The *a priori* selection of the breach parameters (τ_{br} and δ) causes the greatest uncertainty in simulating dam-break flood waves. However, sensitivity studies (Fread, 1980) show that large differences in the discharges near the Teton Dam rapidly diminish in the downstream direction. After 15 miles the variation diminished to (+15 to -8 per cent) for variations in δ of a factor of 2 and in τ_{br} of a factor from 0.3 to 2. The tendency for extreme peak attenuation

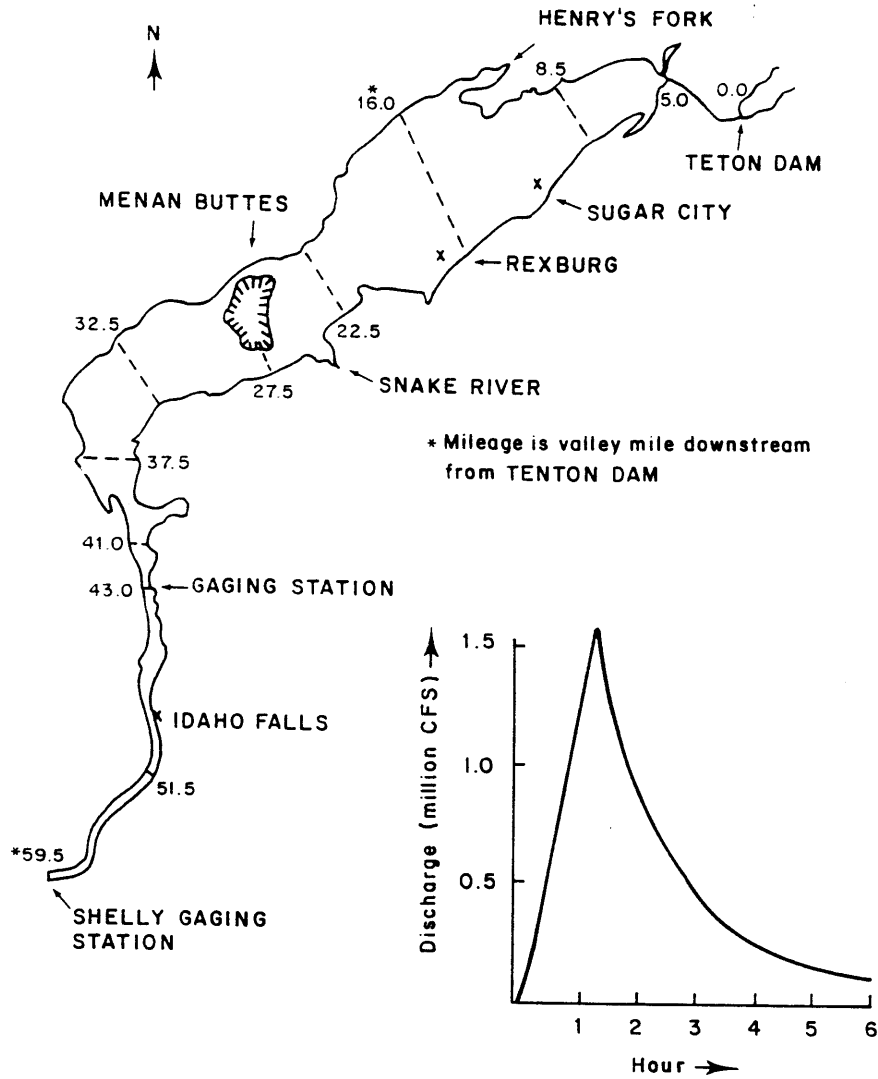


Figure 14.11 Outflow hydrograph and flood area downstream of Teton Dam

and rapid damping of differences in the peak discharge is accentuated in the case of Teton Dam due to the presence of the very wide valley. Had the narrow canyon extended all along the 60-mile reach to the Shelly gauge, the peak discharge would not have attenuated as much and the differences in peak discharges due to variations in δ and τ_{br} would be more persistent. In this instance the peak discharge (cfs) would have attenuated to about 350,000 rather

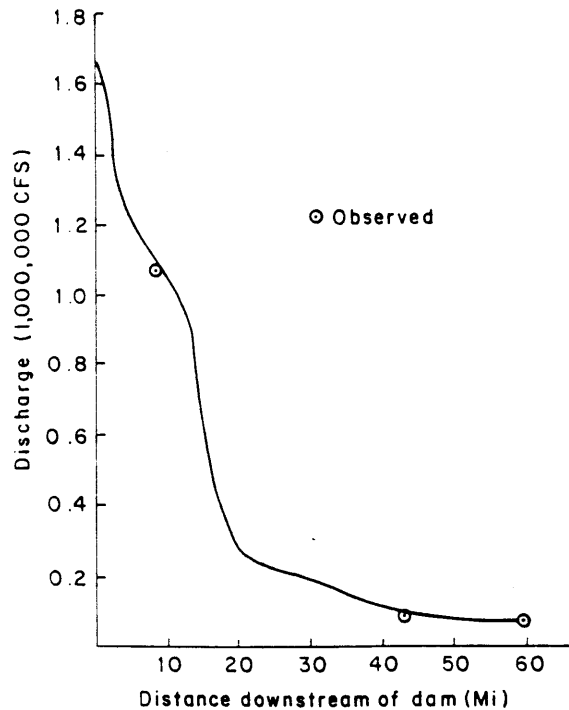


Figure 14.12 Profile of peak discharge from Teton Dam failure

than 67,000 and the differences in peak discharges at mile 59.5 would have been about 27 per cent, as opposed to less than 5 per cent for the actual wide valley.

Computed peak elevations compared favourably with observed values. The average absolute error was 1.5 ft, while the average arithmetic error was only -0.2 ft. The computed travel time of the flood wave was compared with observed values at the locations of the discharge measurements; they differed by less than 10 per cent.

A typical simulation of the Teton flood involved 78 Δx reaches, 55 h of prototype time, and an initial time step (Δt) of 0.06 h which was automatically increased gradually to 0.5 h as the wave propagated downstream and natural dispersion increased the time of rise. Such a simulation run required only 19 s on an IBM 360/195 computer system.

14.22 A VIEW TOWARDS FUTURE DIRECTIONS IN CHANNEL ROUTING

The hydrological models (especially the Muskingum–Cunge model) will continue to be much used, particularly as components of precipitation-runoff

catchment models for routing overland flow and channel flow associated with the network of headwater streams which feed larger, more mild sloping collecting streams. Therefore it is important that the strengths and limitations of the simplified models be set forth and their relationship to other routing models, especially the complete models, be understood through analyses similar to those by Cunge (1969), Miller and Cunge (1975), Ponce *et al.* (1978), and Koussis (1978, 1980). The analysis should quantify a model's characteristics in terminology familiar to hydraulic engineers.

It appears that the trend for increasing computational speed and storage capabilities of both large and small computers will be sustained throughout the 1980s. Also, the accessibility to such computational resources will become more commonplace and economically feasible to both large and small agencies, universities, and engineering consulting firms. For these reasons, and their great range of applicability, flood routing models based on the complete Saint-Venant equations will continue to receive much attention from model developers and increasing use in the engineering community. Since the implicit dynamic models are the most promising of the complete hydraulic models for many flood routing applications due to their superior computational efficiency, many future improvements will likely be associated with this type of model. Some future improvements may include the following: (1) Develop an improved one-dimensional modelling of meandering rivers with short-circuiting floodplain flow and large differences between channel and floodplain properties such as hydraulic roughness and wave celerity; some effort in this area has been made by Radojkovic (1976), Fread (1976), Tingsanchali and Ackermann (1976), and Weiss and Midgley (1978). (2) Analysis of effects of nonlinear terms in the Saint-Venant equations on the stability and accuracy of implicit solution algorithms. (3) Develop manual and/or automatic smoothing techniques to overcome nonlinear instabilities due to rapid variations of cross-sectional properties with elevation and distance along the waterway.

A significant area of general improvement consists of expanding flood routing models to account for significant effects of bridges, breached or overtopped levees, ice covers, ice jams, flow exchanges with groundwater aquifers due to bed and bank seepage and floodplain infiltration, and bed elevation and bed roughness changes caused by sediment transport. There exists a large body of knowledge in each of these areas; however, the incorporation of this into flood routing models has not received enough attention. Some work in this area has been done, e.g. Chen and Simons (1975) and Ponce *et al.* (1979) concerning bed elevation changes due to sediment transport; Pinder and Sauer (1971), Freeze (1972), Hall and Moench (1972), Cooley and Westphal (1974), and Pogge and Chiang (1977) concerning the flow exchange between the waterway and adjacent aquifer; Uzner and Kennedy (1976) concerning ice jams; and Balloffet (1969), Cunge (1975b), Fread (1978, 1980) concerning effects of levees, bridge/embankments, and other man-made structures.

Calibration of flood routing models is most essential for good results. The calibration process for diffusion and dynamic hydraulic models when applied to a complex system of waterways is often time-consuming and requires considerable experience. There is a need for the development of objective calibration methodologies which may be trial-error and/or automatic, e.g., Yeh and Becker (1973), and Fread and Smith (1978).

Flood routing models should be developed having a modular design. This will permit convenient selection of various combinations of external and internal boundary conditions permitting the same model to be used for a wide range of applications.

There is also a need for the development of updating techniques to improve real-time simulation of unsteady flows such as in flood forecasting. Approaches include the use of filter theory, e.g., the Kalman filter technique (Chiu and Isu, 1978).

Automated data processing techniques are needed to allow the inexpensive and rapid development of the cross-section and roughness parameters of the hydraulic-type models. The sources of data should include remote sensing as well as conventional on-site surveys and measurements (Lai *et al.*, 1980).

REFERENCES

- Abbott, M. B. (1966) *An Introduction to the Method of Characteristics*. New York: American Elsevier.
- Abbott, M. B. (1976) 'Discussion of review of models of tidal waters by J. B. Hinwood and I. G. Wallis', *J. Hydraulic Div.*, ASCE, **102** (HY8), 1145-1148.
- Abbott, M. B., and Cunge, J. A. (1975) 'Two-dimensional modeling of tidal deltas and estuaries'. In Mahmood, K., and Yevjevich, V. (eds), *Unsteady Flow in Open Channels*, Fort Collins, Colorado: Water Resources Publications, Chapter 18, pp. 763-812.
- Abbott, M. B., and Ionescu, F. (1967) 'On the numerical computation of nearly horizontal flows'. *J. Hydraulic Res.*, **5**(2), 97-117.
- Amein, M. (1966) 'Streamflow routing on computer by characteristics'. *Water Resources Res.* **2**(1), 123-130.
- Amein, M., and Chu, H. L. (1975) 'Implicit numerical modeling of unsteady flows'. *J. Hydraulic Div.*, ASCE, **101** (HY6), 93-108.
- Amein, M., and Fang, C. S. (1970) 'Implicit flood routing in natural channels'. *J. Hydraulic Div.*, ASCE, **96** (HY12), 2481-2500.
- Balloffet, A. (1969) 'One-dimensional analysis of floods and tides in open channels'. *J. Hydraulic Div.*, ASCE, **95** (HY4), 1429-1451.
- Baltzer, R. A. and Lai, C. (1968) 'Computer simulation of unsteady flow in waterways'. *J. Hydraulic Div.*, ASCE, **94** (HY4), 1083-1117.
- Bennett, J. P. (1975) 'General model to simulate flow in branched estuaries'. In *Symp. on Modeling Techniques*, Vol. I, 2nd Annual Symp. of Waterways, Harbors, and Coastal Engng. Div., ASCE, pp. 643-662.
- Boussinesq, J. (1871) 'Theory of the liquid intumescence, called a solitary wave or a wave of translation, propagated in a channel of rectangular cross section'. *Comptes Rendus Acad. Sci., Paris*, **72**, 755-759.

- Brakensiek, D. L. (1965). 'An implicit flood routing method'. Paper presented at Hydraulic Div. Specialty Conf., ASCE, Tucson, Arizona.
- Chaudhry, Y. M., and Contractor, D. N. (1973) 'Application of implicit method to surges in channels'. *Water Resources Res.*, 9(6), 1605-1612.
- Chen, Y. H., and Simons, D. B. (1975) 'Mathematical modeling of alluvial channels'. In *Symp. on Modeling Techniques*, Vol. 1, 2nd Annual Symp. of Waterways, Harbors, and Coastal Engng. Div., ASCE, pp. 466-483.
- Chiu, C.-L., and Isu, E. O. (1978) 'Kalman filter in open channel flow estimation'. *J. Hydraulic Div.*, ASCE, 104 (HY8), 1137-1152.
- Chow, V. T. (1959) *Open-Channel Hydraulics*, New York: McGraw-Hill Book Co., pp. 601-604.
- Contractor, D. N., and Wiggert, J. M. (1972) *Numerical Studies of Unsteady Flow in the James River*. Bul. 51, VPI-WRRC 51, Water Resources Research Center, Virginia Poly Institute and State Univ., Blacksburg, Virginia.
- Cooley, R. L., and Westphal, J. A. (1974) *An Evaluation of the Theory of Ground-water and River-water Interchange, Winnemucca Reach of the Humbolt River, Nevada*. Tech. Report Series H-W No. 19, Center for Water Resources Research, Desert Research Institute, Reno, Nevada.
- Cooley, R. L., and Moin, S. A. (1976) 'Finite element solution of Saint-Venant equations'. *J. Hydraulic Div.*, ASCE, 102 (HY6), 759-775.
- Cunge, J. A. (1966) *Etude d'un Schema de Differences Finies Applique a l'integration Numerique d'un Certain Type d'equation Hyperbolique d'ecoulement* [Study of a Finite Difference Scheme, Applied to Numerical Integration of the Certain Type of Hyperbolic Flow Equation]. Thesis, Grenoble University, France.
- Cunge, J. A. (1969) 'On the subject of a flood propagation computation method (Muskingum method)'. *J. Hydraulic Res.*, 7(2), 205-230.
- Cunge, J. A. (1975a) 'Rapidly varying flow in power and pumping canals'. In Mahmood, K., and Yevjevich, V. (eds), *Unsteady Flow in Open Channels*, Vol. II. Fort Collins, Colorado: Water Resources Publications, Chapter 14, pp. 539-586.
- Cunge, J. A. (1975b) 'Two-dimensional modeling of flood plains'. In Mahmood, K., and Yevjevich, V. (eds), *Unsteady Flow in Open Channels*, Vol. II. Fort Collins, Colorado: Water Resources Publications, Chapter 17, pp. 705-762.
- Diskin, M. H. (1967) 'On the solution of the Muskingum method of flood routing equation'. *J. Hydrol.*, 5, 286-289.
- Dooge, J. C. I. (1973) *Linear Theory of Hydraulic Systems*, Tech. Bul. No. 1468, USDA Agricultural Research Service, Beltsville, Maryland.
- Dooge, J. C. I., Strupczewski, W. G., and Napiorkowski, J. J. (1982) 'Hydrodynamic derivation of storage parameters of the Muskingum model'. *J. Hydrol.*, 54, 371-387.
- Dronkers, J. J. (1964) *Tidal Computations in Rivers and Coastal Waters*. New York: Interscience Publishers, Inc.
- Dronkers, J. J. (1969) 'Tidal computations for rivers, coastal areas, and seas'. *J. Hydraulic Div.*, ASCE, 95 (HY1), 29-77.
- Ellis, J. (1970) 'Unsteady flow in channel of variable cross section', *J. Hydraulic Div.*, ASCE, 96 (HY10), 1927-1945.
- Fread, D. L. (1971) 'Discussion of implicit flood routing in natural channels by M. Amein and C. S. Fang'. *J. Hydraulic Div.*, ASCE, 97 (HY7), 1156-1159.
- Fread, D. L. (1973) 'Technique for implicit dynamic routing in rivers with tributaries'. *Water Resources Res.*, 9(4), 918-926.
- Fread, D. L. (1974) *Numerical Properties of Implicit Four-point Finite Difference Equations of Unsteady Flow*. NOAA Tech. Memo NWS HYDRO-18, U.S. Department of Commerce, National Weather Service, Silver Spring, Maryland.

- Fread, D. L. (1976) 'Flood routing in meandering rivers with flood plains'. In *Symp. on Inland Waterways for Navigation, Flood Control and Water Diversion*, Vol. I, ASCE, pp. 16-35.
- Fread, D. L. (1978) 'NWS operational dynamic wave model'. In *Verification of Mathematical and Physical Models*, Proc. of 26th Annual Hydr. Div. Specialty Conf., ASCE, College Park, Maryland, pp. 455-464.
- Fread, D. L. (1980) 'Capabilities of NWS model to forecast flash floods caused by dam failures'. In *Proc. of 2nd Conf. on Flash Floods*, Atlanta, Georgia, American Met. Soc., pp. 171-178.
- Fread, D. L. and Smith, G. F. (1978) 'Calibration technique for 1-D unsteady flow models'. *J. Hydraulic Div.*, ASCE, **104** (HY7), 1027-1044.
- Freeze, R. A. (1972). 'Role of subsurface flow in generating surface runoff, 1. Base flow contributions to channel flow'. *Water Resources Res.*, **8**(3), 609-623.
- Garrison, J. M., Granju, J. P. and Price, J. T. (1969) 'Unsteady flow simulation in rivers and reservoirs'. *J. Hydraulic Div.*, ASCE, **95** (HY5), 1559-1576.
- Goodrich, R. D. (1931) 'Rapid calculation of reservoir discharge'. *Civil Eng.*, **1**, 417-418.
- Gray, W. G., Pinder, G. F. and Brebbia, C. A. (1977) *Finite Elements in Water Resources*. London: Pentech Press.
- Greco, F., and Panattoni, L. (1975) 'An implicit method to solve Saint-Venant equations'. *J. Hydraulic.*, **24**, 171-185.
- Grupert, J. P. (1976) 'Numerical computation of two-dimensional flows'. *J. Waterways, Harbors, Coastal Engng. Div.*, ASCE, **102**(WW1), 1-12.
- Gunaratnam, D. J. and Perkins, F. E. (1970) *Numerical Solution of Unsteady Flows in Open Channels*. Hydrodynamic Lab. Report 127, Dept. of Civil Engng., Massachusetts Institute of Technology, Cambridge, Massachusetts.
- Hall, F. R., and Moench, A. F. (1972) 'Application of the convolution equation to stream-aquifer relationships'. *Water Resources Res.*, **8**(2), 487-493.
- Harder, J. A., and Armacost, L. V. (1966) *Wave Propagation in Rivers*. Hydraulic Engng. Lab., Report No. 1, Series 8, University of California, Berkeley, California.
- Harley, B. M. (1967) *Linear Routing in Uniform Channels*. Thesis, University College, Cork, Ireland.
- Harley, B. M., Perkins, F. E., and Eagleson, P. S. (1970) *A Modular Distributed Model of Catchment Dynamics*. Hydrodynamics Lab. Report 133, Department of Civil Engineering, Massachusetts Institute of Technology, Cambridge, Massachusetts.
- Harris, G. S. (1970) 'Real time routing of flood hydrographs in storm sewers'. *J. Hydraulic Div.*, ASCE, **96** (HY6), 1247-1260.
- Harrison, A. S., and Bueltel, C. J. (1973) *Computer Simulation of Missouri River Floods, Part I*, U.S. Army Corps of Engineers, Missouri River Div., Omaha, Nebraska.
- Henderson, F. M. (1966) *Open Channel Flow*. New York: Macmillan Co., pp. 285-287.
- Hinwood, J. B., and Wallis, I. G. (1975a) 'Classification of models of tidal waters'. *J. Hydraulic Div.*, ASCE, **101** (HY10), 1315-1331.
- Hinwood, J. B., and Wallis, I. G. (1975b) 'Review of models of tidal waters'. *J. Hydraulic Div.*, ASCE, **101** (HY11), 1405-1421.
- Isaacson, E., Stoker, J. J., and Troesch, A. (1954) *Numerical Solution of Flood Prediction and River Regulation Problems, Report II*. New York University Institute of Mathematical Science, IMM-205, New York.
- Isaacson, E., Stoker, J. J., and Troesch, A. (1956) *Numerical Solution of Flood*

- Prediction and River Regulation Problems, Report III*. New York University Institute of Mathematical Science, IMM-NYU-235, New York.
- Johnson, B. H. (1974) *Unsteady Flow Computations on the Ohio-Cumberland-Tennessee-Mississippi River System*. Tech. Report H-74-8, Hydraulics Lab., Waterways Experiment Station, US Army Corps of Engineers, Vicksburg, Mississippi.
- Kamphuis, J. W. (1970) 'Mathematical tidal study of St. Lawrence River'. *J. Hydraulic Div.*, ASCE, **96** (HY3), 643-664.
- Keefer, T. N., and McQuivey, R. S. (1974) 'Multiple linearization flow routing model'. *J. Hydrolic Div.*, ASCE, **100** (HY7), 1031-1046.
- Koussis, A. D. (1978) 'Theoretical estimations of flood routing parameters'. *J. Hydraulic Div.*, ASCE, **104** (HY1), 109-115.
- Koussis, A. D. (1980) 'Comparison of Muskingum method difference schemes'. *J. Hydraulic Div.*, ASCE, **106** (HY5), 925-929.
- Lai, C., Schaffranek, R. W., and Baltzer, R. A. (1980) 'An operational system for implementing simulation models: a case study'. In *Proc. of Verification of Mathematical and Physical Models*, 26th Annual Hydrol. Div. Specialty Conf., ASCE, College Park, Maryland, pp. 415-454.
- Laplace, P. S. (1776) *Recherches sur Quelques Points due Systeme du Monde* [Researches on Some Points of World System]. Memoirs, Vol. 9, Acad. Sci., Paris.
- Liggett, J. A., and Woolhiser, D. A. (1967) 'Difference solutions of the shallow-water equation'. *J. Engng. Mech. Div.*, ASCE, **95** (EM2), 39-71.
- Liggett, J. A. (1975) 'Basic equations of unsteady flow'. In Mahmood, K., and Yevjevich, V. (eds), *Unsteady Flow in Open Channels*, Vol. I. Fort Collins, Colorado: Water Resource Publications, Chapter 2, pp. 29-62.
- Liggett, J. A., and Cunge, J. A. (1975) 'Numerical methods of solution of the unsteady flow equations'. In Mahmood, K., and Yevjevich, V. (eds), *Unsteady Flow in Open Channels*, Vol. I. Fort Collins, Colorado: Water Resources Publications, Chapter 4, pp. 89-182.
- Lighthill, M. J., and Whitham, G. B. (1955) 'On kinematic floods, I: Flood movements in long rivers'. In *Proc. Royal Society Lond.*, **A229**, 281-316.
- Lin, J. O., and Soong, H. K. (1979) 'Junction losses in open channel flows'. *Water Resources Res.*, **15**(2), 414-418.
- Linsley, R. K. (1971) *A Critical Review of Currently Available Hydrologic Models for Analysis of Urban Stormwater Runoff*. Report, Hydrocomp International Inc., Palo Alto, California.
- Linsley, R. K., Kohler, M. A., and Paulhus, J. L. H. (1949) *Applied Hydrology*. New York: McGraw Hill Book Co., pp. 502-530.
- Maddaus, W. O. (1969) *A Distributed Linear Representation of Surface Runoff*. Hydrodynamics Lab. Report 115, Massachusetts Institute of Technology, Cambridge, Massachusetts.
- Martin, C. S. and DeFazio, F. G. (1969) 'Open channel surge simulation by digital computer'. *J. Hydraulic Div.*, ASCE, **95** (HY6), 2049-2070.
- McCarthy, G. T. (1938) 'The unit hydrograph and flood routing'. Paper presented at Conf. of the North Atlantic Div. of US Corps of Engineers, New London, Connecticut.
- Miller, W. A., and Cunge, J. A. (1975) 'Simplified equations of unsteady flow'. In Mahmood, K., and Yevjevich, V. (eds) *Unsteady Flow in Open Channels*, Vol. I. Fort Collins, Colorado: Water Resources Publications, Chapter 5, pp. 183-257.
- Miller, W. A., and Yevjevich, V. (1975) *Unsteady Flow in Open Channels*. Bibliography, Vol. III. Fort Collins, Colorado: Water Resources Publications.

- Nash, J. E. (1959) 'A note on the Muskingum method of flood routing'. *J. Geophys. Res.*, **64**, 1053-1056.
- Newton, Sir, I. (1687) 'Propositions'. Book 2 in *Principia*, pp. 44-46, Royal Society, London.
- Pinder, G. F., and Sauer, S. P. (1971) 'Numerical simulation of flood wave modification due to bank storage effects'. *Water Resources Res.*, **7**(1), 63-70.
- Pogge, E. C., and Chiang, W.-L. (1977) *Further Development of a Stream-Aquifer System Model*. Kansas Water Resources Research Institute, University of Kansas, Lawrence, Kansas.
- Poisson, S. D. (1816) *Memoir on the Theory of Waves*. Memoirs, Vol. 1. Acad. Sci., Paris, pp. 71-186.
- Ponce, V. M. (1981). *Development of an Algorithm for the Linearized Diffusion Method of Flood Routing*. SDSU Civil Engineering Series No. 81144, San Diego State University, San Diego, California.
- Ponce, V. M., and Simons, D. B. (1977) 'Shallow wave propagation in open channel flow'. *J. Hydraulic Div., ASCE*, **103** (HY12), 1461-1476.
- Ponce, V. M., and Yevjevich, V. (1978) 'Muskingum-Cunge method with variable parameters'. *J. Hydraulic Div., ASCE*, **104** (HY12), 1663-1667.
- Ponce, V. M., Indlekofer, H., and Simons, D. B. (1979) 'The convergence of implicit bed transient models'. *J. Hydraulic Div., ASCE*, **105** (HY4), 351-363.
- Ponce, V. M., Li, R. M., and Simons, D. B. (1978) 'Applicability of kinematic and diffusion models'. *J. Hydraulic Div., ASCE*, **104** (HY3), 353-360.
- Preissmann, A. (1961) 'Propagation of translatory waves in channels and rivers'. In *Proc., First Congress of French Assoc. for Computation*, Grenoble, France, pp. 433-442.
- Puls, L. G. (1928) *Construction of Flood Routing Curves*. House Document 185, US 70th Congress, 1st session, Washington, DC, pp. 46-52.
- Quick, M. C., and Pipes, A. (1975) 'Nonlinear channel routing by computer'. *J. Hydr. Div., ASCE*, **101** (HY6), 651-664.
- Quinn, F. H., and Wylie, E. B. (1972) 'Transient analysis of the Detroit River by the implicit method'. *Water Resources Res.*, **8**(6), 1461-1469.
- Radojkovic, M. (1976) 'Mathematical modelling of rivers with flood plains'. In *Symp. on Inland Waterways for Navigation, Flood Control and Water Diversions*, Vol. I, ASCE, pp. 56-64.
- Rockwood, D. M. (1958) 'Columbia Basin stream flow routing computer'. *Transactions, ASCE*, **126**(4), 32-56.
- Saint-Venant, B. De (1871) 'Theory of unsteady water flow, with application to river floods and to propagation of tides in river channels'. *Comptes Rendus Acad. Sci., Paris*, **73**, 148-154, 237-240. (Translated into English by US Corps of Engineers, No. 49-g, Waterways Experiment Station, Vicksburg, Mississippi, 1949.)
- Sauer, V. B. (1973) 'Unit-response method of open-channel flood routing'. *J. Hydraulic Div., ASCE*, **99** (HY1), 179-193.
- Singh, V. P., and McCann, R. C. (1980) 'Some notes on Muskingum method of flood routing'. *J. Hydrol.*, **48**(3), 343-361.
- Stoker, J. J. (1953). *Numerical Solution of Flood Prediction and River Regulation Problems; Derivation of Basic Theory and Formulation of Numerical Methods of Attack*. Report I, New York University Institute of Mathematical Science, Report No. IMM-NYU-200, New York.
- Stoker, J. J. (1957). *Water Waves*. New York: Interscience, pp. 452-455.
- Streeter, V. L., and Wylie, E. B. (1967) *Hydraulic Transients*. New York: McGraw Hill Book Co., pp. 239-259.

- Strelkoff, T. (1969) 'The one-dimensional equations of open-channel flow'. *J. Hydraulic Div.*, ASCE, **95** (HY3), 861–874.
- Strelkoff, T. (1970) 'Numerical solution of Saint-Venant equations'. *J. Hydraulic Div.*, ASCE, **96** (HY1), 223–252.
- Strupczewski, W., and Kundzewicz, Z. (1980) 'Translatory characteristics of the Muskingum method of flood routing—a comment'. *J. Hydrol.*, **98**, 363–368.
- Tatum, F. E. (1940) *A Simplified Method of Routing Flood Flows Through Natural Valley Storage*. Unpublished memo, US Engineers Office, Rock Island, Illinois.
- Tingsanchali, T., and Ackermann, N. L. (1976) 'Effects of overbank flow in flood computations'. *J. Hydraulic Div.*, ASCE, **102** (HY7), 1013–1025.
- Uzner, M. S., and Kennedy, J. F. (1976) 'Theoretical model of river ice jams'. *J. Hydraulic Div.*, ASCE, **102** (HY9), 1365–1383.
- Vasiliev, O. F., Gladyshev, M. T., Pritvits, N. A., and Sudobicher, V. G. (1975) 'Methods for the calculation of shock waves in open channels'. In *Proc., 11th Congress IAHR*, Leningrad, USSR, paper 3.44.
- Vicens, G. J., Harley, B. M., and Schaake, J. C. (1975) 'Flow 2D: a two-dimensional flow model for flood plains and estuaries'. In *Symp. Modeling Techniques*, Vol. II. 2nd Annual Symp. of Waterways, Harbors, and Coastal Engng. Div., ASCE, pp. 1487–1504.
- Weinmann, P. E., and Laurenson, E. M. (1979) 'Approximate flood routing methods: a review'. *J. Hydraulic Div.*, ASCE, **105** (HY13), Proc., Paper 15057.
- Weiss, H. W., and Midgley, D. C. (1978) 'Suite of mathematical flood plain models'. *J. Hydraulic Div.*, ASCE, **104** (HY3), 361–376.
- Wooding, R. A. (1965) 'A hydraulic model for the catchment-stream problem, I, kinematic wave theory'. *J. Hydrol.*, **3**.
- Woolhiser, D. A., and Liggett, J. A. (1967) 'Unsteady one-dimensional flow over a plane—the rising hydrograph'. *Water Resources Res.*, **3**(3), 753–771.
- Wylie, E. B. (1970) 'Unsteady free-surface flow computations'. *J. Hydraulic Div.*, ASCE, **96** (HY11), 2241–2251.
- Yeh, W. W.-G. and Becker, L. (1973). 'Linear programming and channel flow identification'. *J. Hydraulic Div.*, ASCE, **99** (HY11), 2013–2021.

